
Innovative controls for renewable source integration into smart energy systems



www.incite-itn.eu

D6.6

Fourth Workshop Proceedings

WP6 – Dissemination and exploitation of results

Grant Agreement no 675318

Lead beneficiary: TU Delft

Date: 31/07/2018

Nature: R

Dissemination level: PU



This project has received funding from the European Union's Horizon 2020 research and innovation programme under Marie Skłodowska-Curie grant agreement No 675318.



 675318	D6.6: Fourth Workshop Proceedings	
	WP6: Dissemination and exploitation of results	Version: v1.0
	Author(s): Bart De Schutter (TUD), Tomas Pippia (TUD), Marta Fonrodona (IREC)	Security: PU

TABLE OF CONTENTS

DOCUMENT HISTORY	4
DEFINITIONS	5
ABBREVIATIONS	6
DISCLAIMER OF WARRANTIES.....	7
EXECUTIVE SUMMARY	8
1. Introduction	9
2. Program.....	10
3. Abstracts.....	13

 675318	D6.6: Fourth Workshop Proceedings	
	WP6: Dissemination and exploitation of results	Version: v1.0
	Author(s): Bart De Schutter (TUD), Tomas Pippia (TUD), Marta Fonrodona (IREC)	Security: PU

DOCUMENT INFORMATION

Grant Agreement Number	675318	Acronym	INCITE	
Full title	Innovative controls for renewable source integration into smart energy systems			
Project URL	www.incite-itn.eu			
Deliverable	D6.6	Title	Fourth Workshop Proceedings	
Work package	WP6	Title	Dissemination and exploitation of results	
Delivery date	Contractual	31/07/2018	Actual	19/07/2018
Status	V1.0		Draft <input type="checkbox"/>	Final <input checked="" type="checkbox"/>
Nature	R ¹ <input checked="" type="checkbox"/>	ADM ² <input type="checkbox"/>	PDE ³ <input type="checkbox"/>	Other ⁴ <input type="checkbox"/>
Dissemination Level	PU ⁵ <input checked="" type="checkbox"/>	CO ⁶ <input type="checkbox"/>	Other ⁷ <input type="checkbox"/>	
Authors (Partner)	Bart De Schutter (TUD), Tomas Pippia (TUD), Marta Fonrodona (IREC)			
Responsible Author	Bart De Schutter	Email	b.deschutter@tudelft.nl	
	Partner	TU Delft	Phone	
Description of the deliverable	This report brings together the abstracts of the scientific presentations that will take place during the 4 th INCITE Workshop (2 nd INCITE Summer School + 4 th INCITE Workshop, TU Delft, Delft, The Netherlands, 9-13 July 2018).			
Key words	Dissemination, Proceedings, Workshop, IRP			

¹ Report

² Administrative (website completion, recruitment completion...)


³ Dissemination and/or exploitation of project results

⁴ Other including coordination

⁵ Public: fully open, e.g. web


⁶ Confidential: restricted to consortium, other designated entities (as appropriate) and Commission services.

⁷ Classified: classified information as intended in Commission Decision 2001/844/EC

 675318	D6.6: Fourth Workshop Proceedings	
	WP6: Dissemination and exploitation of results	Version: v1.0
	Author(s): Bart De Schutter (TUD), Tomas Pippia (TUD), Marta Fonrodona (IREC)	Security: PU


DOCUMENT HISTORY

NAME	DATE	VERSION	DESCRIPTION
Bart De Schutter and Tomas Pippia (TUD), Marta Fonrodona (IREC)	13/07/2018	0.1	First version
Miguel Picallo (EFACEC), Mikel de Prada (IREC)	17/07/2018	0.2	Revisions
Marta Fonrodona (IREC)	19/07/2018	1.0	Final version

 675318	D6.6: Fourth Workshop Proceedings	
	WP6: Dissemination and exploitation of results	Version: v1.0
	Author(s): Bart De Schutter (TUD), Tomas Pippia (TUD), Marta Fonrodona (IREC)	Security: PU


DEFINITIONS

- Beneficiary partners of the INCITE Consortium are referred to herein according to the following codes:
 - **IREC.** Fundacio Institut de Recerca de l'Energia de Catalunya (Spain)
 - **UPC.** Universitat Politècnica de Catalunya (Spain)
 - **TU Delft.** Technische Universiteit Delft (Netherlands)
 - **VITO.** Vlaamse Instelling Voor Technologisch Onderzoek (Belgium)
 - **UniBo.** Universita di Bologna (Italy)
 - **UGA.** Université Grenoble Alpes (France)
 - **Efacec Energia.** Efacec Energia - Maquinas e Equipamentos Electricos SA (Portugal)
- **Beneficiary.** The legal entities, which are signatories of the EC Grant Agreement No. 675318, in particular: IREC, UPC, TU Delft, VITO, UniBo, UGA and Efacec Energia.
- **Consortium.** The INCITE Consortium, comprising the above-mentioned legal entities.
- **Consortium Agreement.** Agreement concluded amongst INCITE Parties for the implementation of the Grant Agreement.
- **Grant Agreement.** The agreement signed between the beneficiaries and the EC for the undertaking of the INCITE project (Grant Agreement n° 675318).
- **Partner Organisation.** Legal Entity that is not signatory to the Grant Agreement and does not employ any Researcher within the Project and namely, 3E NV (Belgium), Politecnico di Torino (Italy) and Tokyo Institute of Technology (Japan).

 675318	D6.6: Fourth Workshop Proceedings	
	WP6: Dissemination and exploitation of results	Version: v1.0
	Author(s): Bart De Schutter (TUD), Tomas Pippia (TUD), Marta Fonrodona (IREC)	Security: PU

ABBREVIATIONS

- **CA.** Consortium Agreement
- **CMO.** Central Management Office
- **EC.** European Commission
- **ESR.** Early Stage Researcher
- **GA.** Grant Agreement
- **INCITE.** Innovative controls for renewable source integration into smart energy systems
- **IRP.** Individual Research Project
- **RES.** Renewable Energy Sources
- **WPs.** Work Packages

 675318	D6.6: Fourth Workshop Proceedings	
	WP6: Dissemination and exploitation of results	Version: v1.0
	Author(s): Bart De Schutter (TUD), Tomas Pippia (TUD), Marta Fonrodona (IREC)	Security: PU

DISCLAIMER OF WARRANTIES


This document has been prepared by INCITE project partners as an account of work carried out within the framework of the contract no 675318.

Neither Project Coordinator, nor any signatory party of INCITE Project Consortium Agreement, nor any person acting on behalf of any of them:

- makes any warranty or representation whatsoever, express or implied,
 - with respect to the use of any information, apparatus, method, process, or similar item disclosed in this document, including merchantability and fitness for a particular purpose, or
 - that such use does not infringe on or interfere with privately owned rights, including any party's intellectual property, or
- that this document is suitable to any particular user's circumstance; or
- assumes responsibility for any damages or other liability whatsoever (including any consequential damages, even if Project Coordinator or any representative of a signatory party of the INCITE Project Consortium Agreement, has been advised of the possibility of such damages) resulting from your selection or use of this document or any information, apparatus, method, process, or similar item disclosed in this document.

INCITE has received funding from the European Union's Horizon 2020 research and innovation programme under Marie Skłodowska-Curie grant agreement No 675318.


The content of this deliverable does not reflect the official opinion of the European Union. Responsibility for the information and views expressed in the deliverable lies entirely with the author(s).

 675318	D6.6: Fourth Workshop Proceedings	
	WP6: Dissemination and exploitation of results	Version: v1.0
	Author(s): Bart De Schutter (TUD), Tomas Pippia (TUD), Marta Fonrodona (IREC)	Security: PU

EXECUTIVE SUMMARY

This report brings together the abstracts of the scientific presentations that will take place during the 2nd INCITE Summer School & 4th INCITE Workshop, which was organised by TU Delft and was held in Delft, The Netherlands, on 9-13 July 2018.

Scientific abstracts include the contributions from the invited speakers, whose lectures provided scientific and complementary skills training for the Early Stage Researchers (ESRs), as well as presentations of the progress on the Individual Research Projects (IRPs) by the ESRs.

 675318	D6.6: Fourth Workshop Proceedings	
	WP6: Dissemination and exploitation of results	Version: v1.0
	Author(s): Bart De Schutter (TUD), Tomas Pippia (TUD), Marta Fonrodona (IREC)	Security: PU

1. INTRODUCTION


The 2nd INCITE Summer School and 4th Workshop was held at the 3mE faculty of TU Delft in Delft (The Netherlands), 9-13 July 2018, and was hosted by TU Delft.

During the Summer School part, training to the INCITE ESRs as well as to other students external to INCITE was focused, scientifically, on the topic of Energy Markets and Smart Grids, with scientific seminars from experts. Complementary skills training consisted in training about entrepreneurship and the formation of technological start-ups, and on how to apply for research grants.

During the Summer School, the INCITE ESRs participated in an “Electricity market game”, provided by Professor Laurens de Vries from the Faculty of Technology, Policy, and Management of TU Delft. The objective of this game was to simulate the decisions made by companies operating in electricity markets. Moreover, Summer School attendants visited The Green Village, an institution related to TU Delft in which new ideas in the field of Smart Grids can be analyzed and tested from a technical, legal, commercial, and societal point of view. The Green Village hosts also the Car as Power Plant project, where ESRs took a test drive on board of one of the fuel cell vehicles available.

During the Workshop part, the INCITE ESRs presented their latest research and the current status of their research projects, including results from the secondments that have already taken place.


Formation about the creation of technological start-ups was provided by the technological incubator Yes!Delft, and the training on how to apply for research grants, focused on the IF Marie Curie Fellowship, was provided by Daphne van de Sande from the Valorisation Center at TU Delft.

 675318	D6.6: Fourth Workshop Proceedings	
	WP6: Dissemination and exploitation of results	Version: v1.0
	Author(s): Bart De Schutter (TUD), Tomas Pippia (TUD), Marta Fonrodona (IREC)	Security: PU

2. PROGRAM


2nd INCITE Summer School (9-11/07/2018)

N°	Topic	Speakers	Time
<i>Monday July 9, 2018</i>			
1	Welcome & Introduction	Bart De Schutter (TU Delft)	11:00 – 11:15
2	Smart algorithms for smart grids	Mathijs de Weerd (TU Delft)	11:15 – 12:30
<i>Lunch</i>			12:30 – 13:30
3	Energy markets and control application for thermal systems	Fjo De Ridder (VITO)	13:30 – 15:00
4	Electricity market game (Presentation)	Laurens de Vries (TU Delft)	15:00 – 16:00
<i>Coffee break</i>			16:00 – 16:30
5	Electricity market game (I)	Laurens de Vries (TU Delft)	16:30 – 18:00
<i>End of Day 1</i>			18:00

 675318	D6.6: Fourth Workshop Proceedings	
	WP6: Dissemination and exploitation of results	Version: v1.0
	Author(s): Bart De Schutter (TUD), Tomas Pippia (TUD), Marta Fonrodona (IREC)	Security: PU

N°	Topic	Speakers	Time
07/10/18			
6	Role of hydrogen in a sustainable energy system	Ad van Wijk (TU Delft)	9:00 – 10:30
<i>Coffee break</i>			10:30 – 11:00
7	Electricity market game (II)	Laurens de Vries (TU Delft)	11:00 – 12:30
<i>Lunch</i>			12:30 – 13:30
8	Co-simulation of smart grids	Miloš Cvetković (TU Delft)	13:30 – 14:45
9	Simulating cyber-physical energy systems	Peter Palensky (TU Delft)	14:45 – 16:00
<i>Coffee break</i>			16:00 – 16:30
10	Electricity market game (III)	Laurens de Vries (TU Delft)	16:30 – 18:00
<i>End of Day 2</i>			18:00


N°	Topic	Speakers	Time
Wednesday July 11, 2018			
11	Simulating a large Dutch regional power distribution grid & real-time neighborhood battery control for grid stabilization	Werner van Westering (Liander)	9:30 – 10:45
<i>Coffee break</i>			10:45 – 11:00
12	Electricity market game (IV)	Laurens de Vries (TU Delft)	11:00 – 12:30
<i>Lunch</i>			12:30 – 13:30
13	Distributed stochastic model predictive control for large-scale smart energy systems	Tamás Keviczky (TU Delft)	13:30 – 15:00
14	Visit to The Green Village	Serge Santoo (The Green Village)	15:00 – 17:00
<i>End of Day 3</i>			17:00

 675318	D6.6: Fourth Workshop Proceedings	
	WP6: Dissemination and exploitation of results	Version: v1.0
	Author(s): Bart De Schutter (TUD), Tomas Pippia (TUD), Marta Fonrodona (IREC)	Security: PU

4th INCITE Workshop (12-13/07/2018)

N°	Topic	Speakers	Time
<i>Thursday July 12, 2018</i>			
1	Welcome	Bart De Schutter (TU Delft)	8:55 – 9:00
2	Peak power demand reduction in machine tools: optimization-based control applied to smart manufacturing systems	Carlos Ocampo-Martinez (UPC)	9:00 – 10:00
3	Presentation about start-ups	Ruben Kranendonk (Yes! Delft)	10:00 – 11:00
<i>Coffee break</i>			11:00 – 11:30
4	ESR Track 3		11:30 – 13:00
<i>Lunch</i>			13:00 – 14:00
5	ESR Track 1		14:00 – 16:00
<i>Coffee break</i>			16:00 – 16:30
6	ESR Interaction / SB Meeting		16:30 – 18:00
<i>End of Day 4</i>			18:00

N°	Topic	Speakers	Time
<i>Friday July 13, 2018</i>			
7	ESR Track 2		9:00 – 10:30
<i>Coffee break</i>			10:30 – 11:00
8	ESR Track 4		11:00 – 13:00
<i>Lunch</i>			13:00 – 14:00
9	Applying for research grants	Daphne van de Sande (Valorisation Center, TU Delft)	14:00 – 15:00
<i>Coffee break</i>			15:00 – 15:30
10	Car as power plant (with test drive)	Farid Alavi (TU Delft)	15:30 – 16:30
11	Q&A, Discussion		16:30 – 18:00
<i>End of the workshop</i>			18:00

 675318	D6.6: Fourth Workshop Proceedings	
	WP6: Dissemination and exploitation of results	Version: v1.0
	Author(s): Bart De Schutter (TUD), Tomas Pippia (TUD), Marta Fonrodona (IREC)	Security: PU

3. ABSTRACTS

In the following pages, the abstracts of the ESR presentations can be found:

WP1. Control strategies for distributed power generation

- IRP1.1 – Improving Resiliency of Distributed Energy Management for Electrical Energy Systems (W. Ananduta)
- IRP1.2 – Real-time Market-based Coordination of Heterogeneous Distributed Energy Resources (H. Abdelghany)
- IRP1.3 – Coordinating Energy Flexibility in the Electricity Distribution Grid (S. Chakraborty)
- IRP1.4 – Warping model predictive control (J. Lago)

WP2. Control strategies for energy storage systems

- IRP2.1 – Use of a marginal CO2 emissions signal to activate the energy flexibility of building thermal loads (T. Péan)
- IRP2.2 – Control and management of energy storage elements in micro-grids (U. Raveendran Nair)
- IRP2.3 – Model Predictive Control Methods for Microgrids (T. Pippia)

WP3. Control strategies for RES integration

- IRP3.1 – A Statistical Physics Approach to Dynamic Coherency (or lack of) in Large HVDC Grids (A. Agbemuko)
- IRP3.2 – A new modelling approach for stabilisation of smart grids (F. Koeth)
- IRP3.3 – Wind farms control strategies for grid support (S. Siniscalchi Minna)

WP4. Monitoring tools and secure operation of smart grids

- IRP4.1 – Multistage Stochastic Optimization Programming for the operation of Local Energy Systems (C. Orozco)
- IRP4.2 – A fault detection and localization method for LV distribution grids (N. Sapountzoglou)
- IRP4.3 – Stochastic Optimal Power Flow in Distribution Grids under Uncertainty from State Estimation (M. Picallo)
- IRP4.4 – A multi-period Optimal Power Flow scheme for Low Voltage Distribution Networks (K. Kotsalos)

Improving Resiliency of Distributed Energy Management for Electrical Energy Systems

ESR: Wicak Ananduta

Advisor: Carlos Ocampo-Martinez

Abstract—Electrical networks with distributed generation units can be regarded as systems of interconnected microgrids. The power management of such a system can be done using a distributed model predictive control (MPC) method. However, some agents might not cooperate for their own benefits. Therefore, a methodology to improve the resiliency of the distributed MPC scheme with respect to certain adversarial actions is investigated.

I. DISTRIBUTED ENERGY MANAGEMENT

In the current development of electrical energy systems, the microgrid concept becomes important, particularly as a basis to manage power flows for electrical systems with distributed sources [1]. A microgrid might consist of distributed generation units, loads, and storage units. Moreover, it is capable to autonomously operate itself, i.e., has a local control unit, which dictates the operation of all components. Furthermore, a microgrid is also expected to be able to operate in the island mode, in which the microgrid is disconnected from the main grid.

By considering the preceding definition, an electrical network might be considered as a group of interconnected microgrids and the power management of this network can be considered as an optimization problem of a multi-agent network. Due to the interconnection among the microgrids (agents), each agent needs to consider the influence of its neighbor on itself and vice versa when managing its power production. In this setup, the energy management problem is suitable to be solved using a distributed approach. In a distributed approach, a group of controllers cooperatively compute their control inputs considering a global objective and respecting coupling as well as local constraints. Furthermore, a distributed approach also requires the controllers to exchange information with each other such that they can agree with control inputs that are optimal.

On the other hand, renewable energy sources introduce intermittency issues and additional uncertainties into the network. The addition of energy storage units is considered as one of the solutions to deal with those issues. However, the local control units must then take into account the slow dynamics of the storage. In a model predictive control (MPC) approach, the dynamics are directly included in the computation and the uncertainties are handled by recomputing the control inputs at each time step in a receding horizon fashion.

A combination of MPC and distributed approaches has been proposed as power management in the literature. In particular, MPC schemes that are based on dual decomposition, alternating direction of multipliers (ADMM), and

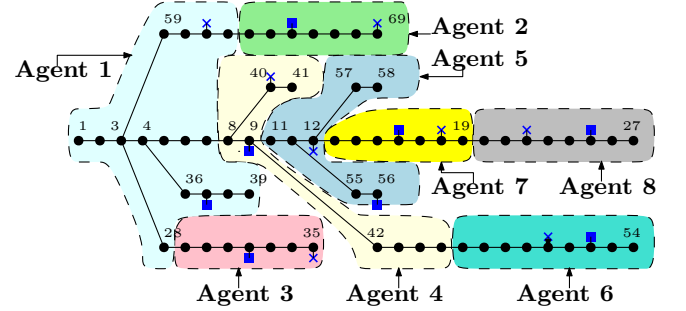


Fig. 1. An example of a distribution network partitioned into a group of interconnected microgrids [2]. Squares indicate the distributed generation units, i.e., ■ and □ represent a renewable generation unit and a dispatchable generator, respectively, whereas crosses, ×, indicate the storages.

optimality condition decomposition (OCD) are some of distributed MPC strategies that have been proposed to deal with power management problems of electrical networks. The main advantage of these strategies is that, given that the problem is convex, the obtained control inputs approximate the optimal solution from solving the problem centrally.

II. HANDLING ADVERSARIAL AGENTS

As previously discussed, the implementation of a distributed MPC strategy requires the cooperation of all agents in the network. Therefore, when some agents do not cooperate, the performance of the system might deteriorate. One possible adversarial behavior is that when some agents do not comply with the control inputs that have been agreed upon among the agents. In this case, although all agents perform the distributed MPC algorithm to compute their control inputs, the agents that do not comply implement control inputs that are different than the computed ones. By doing such actions, these adversarial agents might improve their performances. Moreover, the performance of the other agent degrades. It is worth to mention that very few papers have reported a study on this kind of adversarial actions, e.g., [3] and [4].

Non-compliant actions performed by adversarial agents can be considered as uncertain disturbances affecting the system. Therefore, each regular agent must robustify its control input such that the influence of these uncertainties does not yield to infeasibility. Furthermore, by considering a robust approach, uncertain disturbances of loads and power generation from renewable sources can also be handled at the same time. In a robust approach the worst case of disturbances is considered in the optimization problem.

Therefore, the computed control inputs are feasible regardless the disturbances.

One of the issues that arises when deriving a robust approach is modeling the disturbance. A common assumption used in some robust methods is the knowledge of the bounds of the disturbance. However, such bounds might not be obtainable. One way to deal with this issue is by formulating a chance-constrained program, in which some constraints are allowed to be violated with a predetermined level of violation.

A stochastic method that can solve a chance-constrained problem is called the scenario approach. In this method, a number of uncertainty realizations or scenarios so that the chance constraints can be replaced by a number of hard constraints that use the scenarios. The authors of [5] proposes a two-step stochastic method that is based on the scenario approach. In the first step, probabilistic bounds of the uncertainties are computed using the scenario approach and in the second step, a robust counterpart of the chance-constrained program that uses the probabilistic bounds is solved. This methodology is suitable to be implemented in the power management problem for systems with some non-compliant agents.

In our initial study, we propose a robust program to deal with the attacks [6]. At the moment, we are improving the methodology by implementing the two-step stochastic method in order to deal with the adversarial actions and other uncertainties in the power management problem of interconnected-microgrid systems. Besides being able to compute control inputs that are robustly feasible with respect to the adversarial actions and other uncertainties, the two-step stochastic approach is also useful in the process of identifying the adversarial agents. The probabilistic bounds that are computed in the first step of the stochastic method can also be used to detect an adversarial action. Based on the detection, an identification method that uses Bayesian inference is proposed. Moreover, the proposed identification method also requires each regular agent to solve a local mixed-integer program to determine the connection with its neighbors. Once the adversarial agents are detected, the regular agents can maintain the disconnection from these agents.

III. CONCLUSION

A combination of a robust method and the identification method based on Bayesian inference has been proposed in [6] to deal with non-compliance issues in distributed MPC methods for management of interconnected-microgrid systems. Further investigation to improve the proposed methodology such that it can be implemented in a more general case is needed.

ACKNOWLEDGMENTS

This work has received funding from the European Union's Horizon 2020 research and innovation programme under the Marie Skłodowska-Curie grant agreement No 675318 (INCITE).

REFERENCES

- [1] T. Morstyn, B. Hredzak, and V. G. Agelidis, "Control strategies for microgrids with distributed energy storage systems: An overview," *IEEE Transactions on Smart Grid*, 2016, in press.
- [2] S. A. Arefifar, Y. A. R. I. Mohamed, and T. H. M. El-Fouly, "Supply-adequacy-based optimal construction of microgrids in smart distribution systems," *IEEE Transactions on Smart Grid*, vol. 3, no. 3, pp. 1491–1502, 2012.
- [3] P. Velarde, J. M. Maestre, H. Ishii, and R. R. Negenborn, "Vulnerabilities in Lagrange-based distributed model predictive control," *Optimal Control Applications and Methods*, vol. 39, no. 2, pp. 601–621, 2018.
- [4] D. D. Sharma, S. N. Singh, J. Lin, and E. Foruzan, "Agent-based distributed control schemes for distributed energy storage systems under cyber attacks," *IEEE Transactions on Emerging and Selected Topics in Circuits and Systems*, vol. 7, no. 2, pp. 307–318, 2017.
- [5] K. Margellos, P. Goulart, and J. Lygeros, "On the road between robust optimization and the scenario approach for chance constrained optimization problems," *IEEE Transactions on Automatic Control*, vol. 59, no. 8, pp. 2258–2263, 2014.
- [6] W. Ananduta, J. M. Maestre, C. Ocampo-Martinez, and H. Ishii, "Resilient distributed energy management for systems of interconnected microgrids," in *Proceedings of Conference on Decision and Control*, Miami, USA, 2018, submitted.

Real-time Market-based Coordination of Heterogeneous Distributed Energy Resources

ESR 1.2: Hazem A. Abdelghany, TU Delft

I. INTRODUCTION

This work demonstrates the use of real-time market-based control (RTMBC) to coordinate among numerous, heterogeneous, distributed energy resources (DERs) owned by self-interested users. We use the term “RTMBC” to describe a setting where flexible and inflexible DERs are represented by autonomous agents participating in a spot power market. Agents submit bids/offers that are aggregated and the market is cleared in real time by means of a double auction. Local constraints, objectives and uncertainty are taken into account in the process of bid/offer formulation.

Compared to other coordination techniques, RTMBC provides a degree of end-user privacy and autonomy, scalability, and openness to heterogeneity. However, such a setting usually results in sub-optimal utilization of DERs over time, instability, and inability to guarantee system operability [1]. This is due to the following,

- Decentralization: lack of observable global system state and lack of information about other agents lead to mutually-conflicting decisions [2].
- Real-time operation: lack of planning ahead leads to sub-optimal utilization of resources over multiple time-steps, and sometimes leads to violation of constraints and in-operability of the system [3].

When used for coordination among DERs, these features of RTMBC lead to bulk switching, peak shifting, instability and exhaustion of system flexibility [3], [4].

This work aims at solving the problem of mutually conflicting decisions among different agents in our setting (i.e. synchronous response of decentralized decision makers), and adding a planning ahead feature while maintaining simplicity, privacy and scalability. We investigate the use of RTMBC subject to the constraints imposed by the setting. These are,

- Decentralized decision makers usually have access to small computational capabilities [2], [5].
- Decisions are made in real-time.

Therefore, any solutions employed by the agents in our setting must be computationally and communicationally simple, fast and scalable.

II. MODEL DESCRIPTION

We consider a system with a large number of uninterruptible time-shiftable devices owned by different agents (i.e. flexible loads). Each device has a deadline, duration and constant power consumption. The model also accounts for flexible generation with linearly increasing marginal cost, inflexible load, and inflexible generation which can be curtailed. To solve the optimal coordination problem in settings where central optimization is not possible (i.e. due to privacy, scalability constraints, etc.), we use RTMBC. However, it is required to overcome the problems of mutually conflicting decisions and lack of planning ahead.

We propose a Markov decision process (MDP) based bidding strategy for flexible agents, taking into account probabilistic price forecasts. We show theoretically that identical agents only differentiated by deadlines will never have the same bid. Thus, creating diversity and avoiding the problem of synchronous response (i.e. bulk switching and peak shifting).

Moreover, we implement a test system where it is shown that given probabilistic price forecasts, near-optimal collective behaviour can be achieved.

As a reference solution we assume a central optimizer has complete information about the system, and aims at minimizing the total cost of generation over the planning horizon. In the case of identical flexible loads only differentiated by deadlines, the optimal coordination problem can be modelled and solved as a Mixed Integer Quadratic Program (MIQP).

REFERENCES

- [1] J. D. Thomas and K. Sycara, “Heterogeneity, stability, and efficiency in distributed systems,” in *Proceedings International Conference on Multi Agent Systems*, Jul 1998, pp. 293–300.
- [2] J. Pasquale, “Problems of decentralized control: Using randomized coordination to deal with uncertainty and avoid conflicts,” in *Coordination Theory and Collaboration Technology*. Psychology Press, 2013, pp. 369–389.
- [3] M. H. Syed, P. Crolla, G. M. Burt, and J. K. Kok, “Ancillary service provision by demand side management: A real-time power hardware-in-the-loop co-simulation demonstration,” in *2015 International Symposium on Smart Electric Distribution Systems and Technologies (EDST)*, Sep. 2015, pp. 492–498.
- [4] A. van der Veen, “Connecting PowerMatcher to the electricity markets: an analysis of a Smart Grid application,” Ph.D. dissertation, TNO, Aug. 2015.
- [5] A. Molderink, V. Bakker, M. G. C. Bosman, J. L. Hurink, and G. J. M. Smit, “On the effects of MPC on a domestic energy efficiency optimization methodology,” in *2010 IEEE International Energy Conference*. IEEE, Dec. 2010.



Coordinating Energy Flexibility in the Electricity Distribution Grid

Shantanu T. Chakraborty, Remco Verzijlbergh, Zofia Lukszo

Abstract— To reliably operate an electricity distribution grid with a high penetration of RES, system operators need flexible resources that provide the functionalities of storing energy or modifying use, and reacting quickly to meet required operating levels. While at the industrial consumer level, demand response has resulted in significant reductions in energy demand, the provision of demand-side flexibility at the residential and commercial consumer level, remains an area of active research that is currently being explored.

Energy flexibility through aggregator function is expected to provide services to the DSO for addressing issues of congestion management, voltage regulation and accounting for line losses at the distribution grid. End-customers at the distribution grid can also benefit from their interactions with the DSO and aggregators to hedge against electricity price volatility. The DSOs can be viewed as key players for enabling a successful energy transition, in which they are expected to guarantee distribution system stability, power quality, technical efficiency and cost effectiveness in a smart grid that has a high integration of variable RES generators. For accomplishing its goal, coordination between the DSO and aggregators is crucial and further clarity on this topic is required. In the light of this requirement, the purpose of this project is to shed light on the coordination of energy flexibility between the DSO, aggregators, and end-customers in a future electricity grid that has a high integration of RES.

I. INTRODUCTION

Large scale integration of distributed energy sources, such as wind and solar, pose both advantages and challenges in the power system. While it positively contributes to the reduction of carbon footprint of electricity, its intermittent nature leads to a high level of uncertainty and variability in the management of the grid. Price volatility [1], voltage deviations and congestion management [2] are a few of the issues that arise due to the variability. Increasing energy flexibility at the distribution grid is viewed as one of the possible solutions to address the issues emerging from high integration of RES. Aggregators provide an opportunity to aggregate flexibility provision from small-scale residential and commercial consumers and offer these flexibility services to the system operators such as the Transmission System Operator (TSO) and Distribution System Operator (DSO) through markets such as ancillary service markets or through bilateral contracts.

Hence, an important cornerstone of this project is to investigate the coordination of energy flexibility between DSO, aggregator, and end-customers in a future electricity

distribution grid that has a high integration of RES. The rest of the abstract is organized as follows; Section II provides a literature review and identified research gap, Section III presents the research proposal and planned methods.

II. COORDINATING FLEXIBILITY: STATE-OF-THE-ART

From literature, previous works on coordinating energy flexibility at the distribution grid have mostly considered either the DSO perspective only or only that of the market-driven aggregator [3]. In our research, we focus on the two perspectives simultaneously. There are several knowledge gaps identified in literature regarding coordination of energy flexibility which will be addressed in the course of this research.

Firstly, it is observed from previous works that the aggregators are primarily concerned with maximizing their profits while the impact of their actions on the distribution grid are largely not considered. In addition, the possibility of the aggregator to provide hedging against price volatility by using flexibility has received limited attention [4].

Secondly, currently there is limited knowledge available regarding institutional arrangements that facilitate the coordination between DSO, aggregators, and end-customers, and their impacts on the distribution grid operation. Market mechanisms for local flexibility markets [5], quota based models [6], grid capacities [7] have been theorized, but they lack a mathematical formalism, without which it would be challenging to perform a quantitative assessment of the coordination mechanism in terms of voltage profiles, grid congestions and line losses.

Finally, in the future, it is expected that more aggregators would connect to the grid. In such a distribution grid, the DSO will be required to coordinate with multiple aggregators. Previous studies on this topic have assumed a hierarchical centralized approach [8] for minimizing network operation costs and reducing network peak loads. However, in such an approach aggregators are required to share sensitive information with each other, which could compromise privacy of aggregator operations and their customer profiles. Furthermore, in previous studies, simple models of the distribution grid have been assumed which are not able to account for power losses and congestions in the distribution grid.

Hence, we would like to summarize our research with the main research question, “*What coordination strategies are required between DSO and aggregators in a future electricity distribution grid with high RES penetration to address issues of price volatility, voltage regulation, congestion management and accounting for line losses?*”

* This work has received funding from the European Union’s Horizon 2020 research and innovation programme under the Marie Skłodowska-Curie grant agreement No 675318 (INCITE).

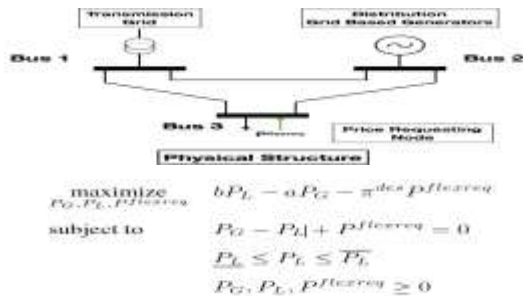
Shantanu T. Chakraborty, Remco Verzijlbergh, Zofia Lukszo are with Delft University of Technology’s Faculty of Technology, Policy and Management (e-mail: S.T.Chakraborty@tudelft.nl, R.A.Verzijlbergh@tudelft.nl, Z.Lukszo@tudelft.nl).

III. RESEARCH PROPOSAL AND PLANNED METHODS

A. Using Flexibility to Hedge Electricity Price Volatility

To address our main research question, we will break down the problem formulation into multiple steps. The first step, is to determine a possible strategy for coordinating flexibility between DSO, aggregator and end-customers to hedge against electricity price volatility while accounting for energy costs and grid constraints [9].

For doing so, we make use of Locational Marginal Prices (LMP) which is a dual variable associated with supply-demand matching. The LMP represents the price that is paid by a customer at a given location, and in recent times has become highly volatile due to increased integration of RES that are intermittent. Motivated by this problem, our research conducted in [10] constrains dual variable in an optimal power flow (OPF) formulation to determine the amount of flexibility required to limit the rise of LMP. In our research, we propose an organizational structure for flexibility management, in which an end-customer can specify its maximum willingness to pay for electricity and through the coordination between the DSO and aggregator the flexibility required for satisfying the price constraints can be provisioned. A pictorial view of the problem setup is as follows:



In the above equation, P_G and P_L represent the magnitude of power generation and load consumption. P^{flexreq} corresponds to the magnitude of flexibility required to ensure that the LMP at node 3 is less than or equal to the maximum willingness to pay for electricity of the end-customer which is specified value as “ π^{des} ”. The main novelty of this approach is that it investigates the possibility of using flexibility to hedge electricity price volatility due to increased integration of RES. Furthermore, we propose a new demand side bidding strategy that is based on price only bids and incorporate them directly into the optimization problem. Future work will focus on different contractual arrangements for flexibility management, incorporating inter-temporal constraints and including line losses in the computation of the LMP.

B. Co-Simulation of Fuel Cell Electric Vehicles

Using the institutional arrangement conceptualized and depicted here, we focus on quantifying the impacts of this arrangement on the operation of the grid. For doing so, we will use a co-simulation based approach, in which we consider a fuel-cell based electric vehicle (FCEV) aggregator in the context of urban areas, that comprise of both commercial and residential loads.



We use a co-simulation environment, in which the social layer comprising of data models for prosumers, consumers, aggregators and DSO with the technical components of the grid which are modeled using Simulink are coupled. The developed model will be executed using real-time digital simulators, and through this setup we will investigate the coordination of increased integration of PV in the distribution grid with flexibility provided by EVs. Furthermore, we investigate the impact that different ownership structures car-sharing/private ownership has on flexibility provision. The main output of this research will be smart charging strategies for FCEVs for addressing issues of voltage regulation, congestion management and line losses using centralized and fully distributed optimization.

C. Distributed Optimization for Flexibility Coordination

Fully distributed optimization will be used for extending the simulation to account for multiple aggregators and price requesting loads. The chosen approach, enables us to address issues of scalability and ensuring data privacy. A benchmark implementation is provided in [11] and work on adapting the problem formulation to account for different network configurations and reducing the number of iterations required for convergence, and asynchronous communication will be published shortly. These developed models will be tested on Representative Network Models [12] to quantify flexibility required and optimize network performance.

REFERENCES

- [1] T. Rintamäki, A.S. Siddiqui, and A.Salo, “Does renewable energy generation decrease the volatility of electricity prices? An analysis of Denmark and Germany”, *Energy Economics*, 2017
- [2] California ISO, “California ISO Duck Curve”, 2013
- [3] R.J. Bessa, M.A.Matos, F.J. Soares and J.A.P. Lopes, “Optimized bidding of a EV aggregation agent in the electricity market”, *IEEE Transactions on Smart Grid*, 2012
- [4] D.P. Zhou, M.A. Dahleh, and C.J. Tomlin, “Hedging Strategies for Load Serving Entities in Wholesale Electricity Markets”, 2017 56th IEEE Conference on Decision and Control (CDC), 2017
- [5] H. Gerard, E. Rivero and D. Six, “Basic schemes for TSO – DSO coordination and ancillary services provision”, 2016
- [6] Nabe, “Smart-Market-Design in deutschen Verteilnetzen”, 2017
- [7] R.A. Verzijlbergh, L.J. De Vries and Z. Lukszo, “Renewable energy sources and responsive demand. Do we need congestion management in the distribution grid?” *IEEE Transactions on Power Systems*, 2014
- [8] Z. Xu, Z. Hu, Y. Song, W. Zhao and Y. Zhang, “Coordination of PEVs charging across multiple aggregators”, *Applied Energy*, 2014.
- [9] K. Baker, “Directly Constraining Marginal Prices”, *IEEE Power Engineering Letters*, 2016.
- [10] S. Chakraborty, R.A. Verzijlbergh, M. Cvetkovic, Z. Lukszo, “Using Flexibility to Hedge Electricity Price Volatility in the Distribution Grid”, *HICSS 2019** (under review)
- [11] S. Karambelkar, L. Mackay, S. Chakraborty, L. Ramirez-Elizondo, P. Bauer, “Distributed Optimal Power Flow for DC Distribution Grids”, In review, PES General Meeting 2018.
- [12] G. Pretticco, F. Gangale, A. Mengolini, A. Lucas and G. Fulli, “Distribution System Operators Observatory: From European Electricity Distribution System to Representative Distribution Networks”, 2016

Warping model predictive control

Jesus Lago

I. INTRODUCTION

In most advanced control processes, the plant optimization is typically divided into two levels: a first level where the plant optimal operational steady-state is computed and a second level that receives the operational point and regulates the plant [1]. One choice to implement the second level is *nonlinear model predictive control (NMPC)* [1], a control scheme that uses the plant model to track the operational setpoints. A variant of this algorithm is a scheme that, instead of computing and tracking a steady-state point, considers a time-varying optimal trajectory. In this scenario, if the second level uses NMPC to track the optimized trajectory, the resultant control scheme is known as *tracking NMPC* [1].

A field where this control scheme is especially relevant is *airborne wind energy (AWE)* [2], a novel type of renewable energy that harvests energy from the wind using flying kites or planes. In order to maximize the harvested energy from the wind, the airfoils have to fly optimal trajectories. In this scenario, assuming that the flying trajectories can be computed offline, tracking NMPC offers a fast and feasible solution to maximize the harvested energy and help AWE system to be integrated in the electrical grid.

II. MOTIVATION AND CONTRIBUTIONS

While stability theory for tracking NMPC has been developed [1] and despite the algorithm being successfully implemented in different scenarios, it suffers from various issues. First, if the trajectories are computed offline, the controller lacks online adaptation to real disturbances and model mismatches. Second, even if the tracking trajectories are recomputed online, the time required to compute a new optimal trajectory introduces delays between the first and the second level [1]; if the system has fast dynamics, these delays prevent the first level to react in time to environmental changes. In both scenarios, if the environmental conditions change, the precomputed trajectory might no longer be optimal nor even feasible.

A field where these problems are especially relevant is AWE as the energy extracted is dependent on the flight trajectory and the trajectory depends in turn on the wind velocity and direction. As these two atmospheric properties vary in the matter of seconds, any controller that aims at optimally flying an AWE system needs to perform online generation of flying trajectories. However, considering that the models proposed for AWE systems [3], [4], [5] typically consist of a state space with 4–15 states and highly nonlinear dynamics, obtaining optimal trajectories is not trivial: complex nonlinear optimization problems need to be solved [5],

[4], which not only require long computation times, but can even lead to failures of the optimization solvers [4]. In this scenario, tracking NMPC becomes unstable and suboptimal.

In this paper, to address the mentioned problems, we present warping NMPC, a control algorithm that tracks optimal trajectories that are updated online at no computational cost. The algorithm is based on warping theory [6], a framework that is based on two key concepts: warpable systems and warpable optimal control problems. The contributions of the paper are 2:

- 1) An algorithm, i.e. warping NMPC, that uses the defined theory to implement a tracking NMPC scheme that computes optimal trajectories in real time.
- 2) Application of the algorithm to the simulation of a real system, i.e. an AWE system, showing how the control algorithm can, under real life conditions, track optimal trajectories that change in time.

III. CONCEPTUAL IDEA OF WARPING

For the considered AWE system, if its optimal trajectories are regarded as a function of the wind speed v_w , a very interesting phenomenon can be observed: as depicted in Figure 1, the periodic optimal trajectories at different wind speeds represent the same 3D flight paths.

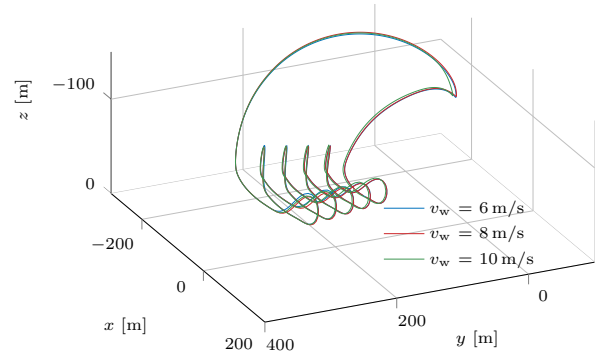


Fig. 1: 3D views of the optimal trajectories for different v_w values.

However, when these trajectories are regarded in the time domain, it can be observed how, while all optimal trajectories make the kite fly through the same physical locations, the velocity of the kite at each trajectory is different. More specifically, while the trajectories are the same, the time it takes for the kite to fly them is dependent on the wind velocity. This effect can be further explained looking at Figure 2, which illustrates the periodic optimal trajectories of two of the states for different wind speeds and in different time frames.

As these trajectories are the same in the 3D space but different in the time domain, they can be interpreted as

*This research has received funding from the European Unions Horizon 2020 research and innovation programme under the Marie Skłodowska-Curie grant agreement No 675318 (INCITE).

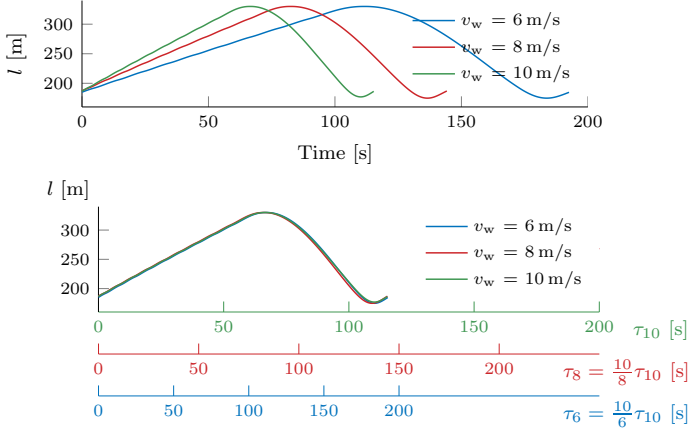


Fig. 2: Top: Optimal tether length l for different v_w values. Bottom: optimal l for different v_w values but defined at three different time frames.

time warped versions of each other. In particular, an optimal trajectory for a certain wind speed could be obtained by squeezing or extending, i.e., warping in time, the optimal trajectory at any other given wind speed. This concept of translating between optimal trajectories at different wind speeds is defined as warping, and it is the basic concept underlying the warping NMPC model.

IV. WARPING NMPC

The proposed algorithm uses the theoretical foundations of warping theory to build a tracking NMPC scheme that can compute tracking trajectories in real time. While the details of the algorithm are out of the scope of this abstract, the basic scheme goes as follows:

- 1) Select a reference parameter/disturbance p_{ref} , e.g. v_w in the AWE system, and compute the optimal trajectory $Y^*(p_{\text{ref}})$ w.r.t. to it.
- 2) Measure the real parameter p , and obtain the optimal trajectory for $Y^*(p)$ by warping in time $Y^*(p_{\text{ref}})$.
- 3) Use the warped trajectory as a tracking trajectory in tracking NMPC.
- 4) Repeat this process at each control time step.

V. CASE STUDY

To test the proposed control scheme, the algorithm is tested using the realistic plant simulator developed by the AWE company Skysails. As a test case, we consider the Skysails kite harvesting energy under a realistic wind speed profile that drops in 25 minutes from 10 m/s to 6 m/s and we compare warping NMPC against a normal tracking NMPC scheme that uses a constant tracking trajectory generated at $v_w = 10$ m/s. The comparison is illustrated in Fig. 3, which depicts the 3D pumping cycle trajectories at the end of the simulation interval, and Table I, which compares the efficiency of the two control schemes in the last pumping cycle.

Considering the obtained results, the following observations can be made:

TABLE I: Warping NMPC comparison considering a nominal wind speed profile decrease from 10 m/s to 6 m/s.

NMPC Scheme	Lloyd Efficiency (maximum 35%)
Tracking NMPC	-3.41 %
Warping NMPC	30.47 %

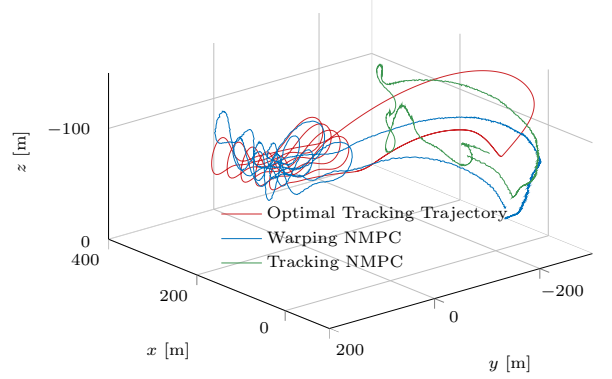


Fig. 3: Comparison between normal NMPC and warping NMPC in a real plant simulator.

- 1) Due to the disturbances, tracking NMPC is unable to harvest any energy, i.e. it displays a negative efficiency.
- 2) By contrast, warping NMPC obtains an efficiency of 30.47 %, which is very close to the ideal 35%.
- 3) Warping NMPC not only obtains a good efficiency, but it is also able to keep the flying trajectories very close to the optimal one.

VI. CONCLUSION

Warping NMPC was presented as a NMPC scheme that allows tracking optimal trajectories at the same computational cost as tracking NMPC. Using a AWE system we have shown that, while a traditional tracking NMPC fails to harvest energy and makes the system unstable, warping NMPC obtains a nearly ideal performance and keeps the system in a periodic and stable trajectory.

REFERENCES

- [1] J. B. Rawlings and R. Amrit, "Optimizing process economic performance using model predictive control," in *Nonlinear Model Predictive Control: Towards New Challenging Applications*. Springer Berlin Heidelberg, 2009, pp. 119–138.
- [2] U. Ahrens, M. Diehl, and R. Schmehl, Eds., *Airborne Wind Energy*. Springer-Verlag Berlin Heidelberg, 2013.
- [3] M. Erhard and H. Strauch, "Theory and experimental validation of a simple comprehensible model of tethered kite dynamics used for controller design," in *Airborne Wind Energy*. Springer, 2013, ch. 8, pp. 141–165.
- [4] S. Gros, M. Zanon, and M. Diehl, "A Relaxation Strategy for the Optimization of Airborne Wind Energy Systems," in *Proceedings of the European Control Conference (ECC)*, 2013, pp. 1011–1016.
- [5] M. Erhard, G. Horn, and M. Diehl, "A quaternion-based model for optimal control of an airborne wind energy system," *ZAMM - Journal of Applied Mathematics and Mechanics*, vol. 97, no. 1, pp. 7–24, 2017.
- [6] J. Lago, M. Erhard, and M. Diehl, "Warping NMPC for online generation and tracking of optimal trajectories," *IFAC-PapersOnLine*, vol. 50, no. 1, pp. 13 252–13 257, 2017.

Use of a marginal CO₂ emissions signal to activate the energy flexibility of building thermal loads

E.S.R.2.1. Thibault Péan

Supervisors: Jaume Salom (IREC) and Ramon Costa-Castelló (UPC)

I. INTRODUCTION

Demand-side management (DSM) consists in acting on the loads rather than on the generation side, in order to ensure the stability of the electrical grid. Such operation can be triggered with different input signals such as the electricity price, the CO₂ emissions of the energy mix, the residual load of the grid, or even combinations of these parameters. DSM control strategies will then intend to shift the loads to periods where the input signal presents a more favorable situation (a lower price for example).

In the literature, the impacts of DSM strategies in terms of CO₂ emissions are usually calculated with average values. In the present work, the marginal emissions factor (MEF) has been used, which provides a more accurate calculation of the CO₂ emissions savings due to DSM interventions. The marginal emissions correspond to the quantity of CO₂ emissions which are avoided for every kWh of electricity saved at a certain moment. It highly depends on the national context and the energy mix of a country [1].

II. DESIGN OF A MARGINAL CO₂ EMISSIONS SIGNAL

To calculate the MEF at national scale in Spain, the following steps have been followed: firstly, the hourly data of the energy mix have been retrieved from the Transmission System Operator (TSO) [2]. The data contains the breakdown of the electricity production for every hour, detailed per energy source. Considering the CO₂ emission coefficients of each energy source [3]¹, the average CO₂ emission factor (EF, in kgCO₂/kWh) can be computed for every hour of the year. Secondly, two time series are calculated: the difference in the system load and the difference in the average CO₂ emissions, from one data point to the next. These data are represented as a scatter plot in Figure 1.

From this figure, the overall MEF can be derived: it corresponds to the slope of the linear regression, here 0.238 kgCO₂/kWh (for comparison, the average MEF found by [1] for Great Britain was 0.69 kgCO₂/kWh). However, it is observed in Figure 1 that the data points are relatively scattered. In fact the MEF varies substantially at different scales, both seasonally and according to the system load, the time of the day or the proportion of renewable energy sources (RES) in the energy mix. For this reason, the data points of Figure 1 have been clustered according to the following rules:

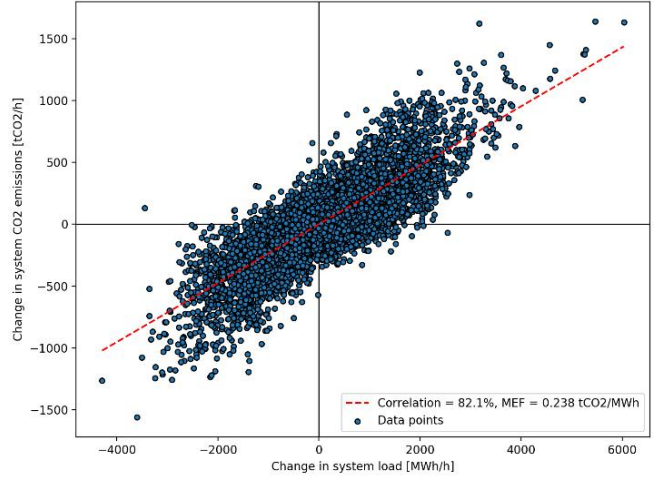


Figure 1. Average MEF (0.238 tCO₂/MWh) in the Spanish electricity mix, based on hourly data from 2016.

- First the data are clustered per ascending system load, into 10 clusters of equal size (same number of data points),
- Inside these 10 datasets, the data are then clustered per proportion of RES (from 10% to 70% and with steps of 10%), with at least 50 points.
- For the data points of each obtained cluster, a linear regression similar to the one presented in Figure 1 is realized, to obtain the MEF of the cluster.

The resulting MEF values are plotted in Figure 2 with colour mapping, in function of both the average system load and the RES share of the clusters. These MEF values have been obtained with an average correlation coefficient of 76% in the different clusters, thus the linear regression results are considered reliable.

Figure 2 clearly demonstrates the dependency of the CO₂ MEF with the RES share and the national load. When both the RES and the load are low, the MEF reaches higher values, because the remaining base load must be covered with CO₂ emitting sources. At middle load levels and high RES share, the MEF displays its lowest values: at these points, there is enough margin to increase the load and benefit from the high availability of renewable sources. Finally, when the load is

T.Q. Péan is with the Catalonia Institute for Energy Research (IREC), Jardins de les Dones de Negre 1, 08930 Sant Adrià de Besòs (Barcelona), Spain (e-mail: tpean@irec.cat).

J. Salom is also with the Catalonia Institute for Energy Research (IREC) (e-mail: jsalom@irec.cat).

R. Costa-Castelló is with the Automatic Control Department, Universitat Politècnica de Catalunya (UPC), C/ Pau Gargallo 5, 08028 Barcelona, Spain (e-mail: ramon.costa@upc.edu).

¹ NB: the emissions of the electricity imported/exported with the neighbouring countries were not considered, as the overall CO₂ emission of these countries was not available. It is believed this would only have a limited impact on the results.

high, the dependency of the MEF on the RES share tends to disappear.

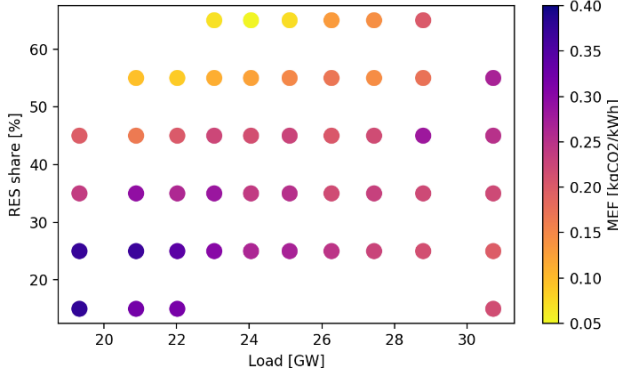


Figure 2. MEF calculated per clusters of RES share and system load (data for Spain from 2016).

To obtain a more direct expression of the MEF, a quadratic fit is derived from the data points presented in Figure 2. The equation of this model is shown in (1), with L the system load (GW), R the RES share (%) and a_i the fitting coefficients. The comparison between the model and the data points is represented in Figure 3. The model is fitted by minimizing the root mean square error (RMSE), which reaches the value of $RMSE = 0.00062 \text{ kgCO}_2/\text{kWh}$ or as a normalized value: $NRMSE = 0.28\%$.

$$MEF = a_0 + a_1R + a_2L + a_3R^2 + a_4L^2 + a_5R \cdot L \quad (1)$$

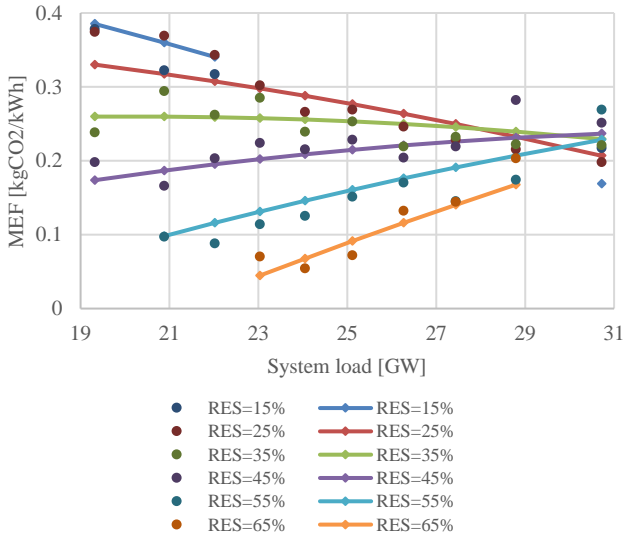


Figure 3. Quadratic model of the MEF in function of the RES share and the system load. The data points (same than Figure 2) are only shown as dots, while the model is represented with solid lines of a similar colour.

When analysing a particular period of time, the MEF can then be obtained by applying (1) to the time series of the power grid. An example is represented in Figure 4: the system load and the RES share enable to calculate the MEF thanks to the quadratic fit equation. The MEF and the average EF curves globally follow the same trends. However, the MEF displays variations of larger amplitude than the average EF, and therefore leaves more room for optimization, which is the main reason behind the whole MEF signal calculation.

To interpret the curves, it should be reminded that a low MEF corresponds to a favourable case to use electricity (the related CO₂ emissions will be lower), while a high MEF will trigger higher emissions. It should be noted that for instance, the MEF signal shows a clear valley around midday. This situation is foreseen to amplify in the future: in [4], the authors have analysed the energy mix of Spain in 2030 and deduced that it will be more profitable to use energy during day hours for a grid-optimal scenario (i.e. when the residual load is negative, due to the importance of solar-based energy).

These statements are highly dependent on the country, the energy mix, and the dispatching of the energy sources within the grid. The operation of the grid also influences greatly the MEF calculation: for instance in Spain, mainly hydropower and gas are used to absorb the daily load fluctuations, while another management strategy would probably lead to different results in terms of marginal emissions.

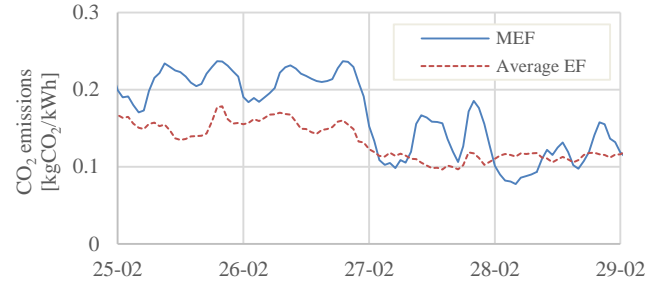


Figure 4. Time series of both the CO₂ EF and MEF, for a few days of February 2016.

III. CONCLUSION

The calculation method of the MEF is validated through the presented study, and the signal was obtained for the Spanish case. Further tests have been carried out using this signal as an input for rule-based control strategies aiming to reduce the CO₂ emissions of building thermal loads (supplied with heat pumps), hence unlocking their flexibility potential.

ACKNOWLEDGMENT

This project has received funding from the European Union's Horizon 2020 research and innovation programme under the Marie Skłodowska-Curie grant agreement No 675318 (INCITE).

REFERENCES

- [1] A. D. Hawkes, "Estimating marginal CO₂ emissions rates for national electricity systems," *Energy Policy*, vol. 38, no. 10, pp. 5977–5987, 2010.
- [2] Red Eléctrica de España, "ESIOS – Sistema de información del operador del sistema," 2018. [Online]. Available: <https://www.esios.ree.es/en> (accessed 07/03/2018). [Accessed: 04-Apr-2017].
- [3] IPCC Working Group III, "Annex III: Technology-specific cost and performance parameters - IPCC," in *Climate Change 2014: Mitigation of Climate Change*, 5th Assess., 2014.
- [4] K. Klein, S. Killinger, D. Fischer, C. Streuling, J. Salom, and E. Cubi, "Comparison of the future residual load in fifteen countries and requirements to grid-supportive building operation," in *Eurosun 2016*, 2016, no. October, pp. 11–14.

Control and management of energy storage elements in micro-grids

Unnikrishnan Raveendran Nair, Ramon Costa-Castelló
Institut de Robotica i Informatica Industrial, CSIC-UPC, Barcelona

Abstract—Energy storage systems are becoming an integral part of the present day grids in aiding the penetration of renewable energy sources. An effective control strategy for storage systems is essential in the effective integration of such systems. An overview of the control architecture and a low level controller for energy storage systems is presented here.

I. INTRODUCTION

The paradigm shift of the electric power system from its reliance on fossil fuels as energy sources to renewable sources have been contributed by the increasing price of the fossil fuels, the various government policies, incentives and protocols for capping carbon emissions [1] [2] [3]. Therefore, modern electric network is seeing a major overhaul by shifting from the traditional centralised to distributed generation. The distributed generation through renewable energy sources(wind, solar) add varying, fluctuating power into the grid, independent of the demand, which can affect the grid stability if the supply demand balance is not met. They also reduce the inertia of the grid due to the absence of any rotational inertia making the grid more susceptible to instabilities during events of sudden load change. The increased drive to incorporate more renewable sources into the grid therefore demands integration of Energy Storage Systems(ESS) in the grid which ensures supply-demand balance, spinning reserves and improved grid inertia [5] [6].

This paper presents an overview of the work done so far in relation to the research work of ESR2.2 in the INCITE project. The objective is developing a control system that ensures stable and efficient integration of ESS in the electric grids. Some results in the primary and secondary control levels for integration of ESS in microgrids is presented here.

II. CONTROL ARCHITECTURE FOR STORAGE SYSTEMS

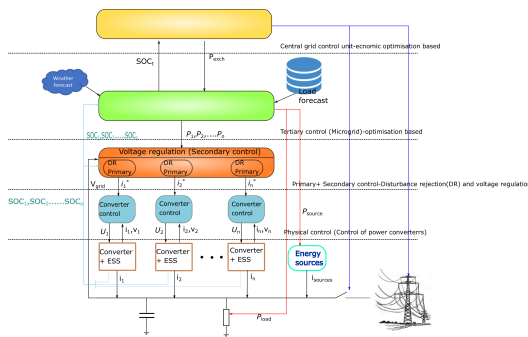


Fig. 1. Control architecture for the ESS

The Fig.1 shows control architecture for ESS considered by the ESR for the integration of ESS into grids. The

hierarchical control scheme has the system divided into three levels: physical control level, primary+secondary, tertiary and central grid control unit.

Physical control level: This level deals with control of power converters which are interfacing the ESS to grids. These converters are required to respond fast to ensure minimum variation in grid parameters. The fast flat response will be ideal to improve the power quality. The controllers at this level should be capable of such a response.

The primary level: This level is responsible for ensuring disturbance rejection in the microgrid. In an interconnected system like the microgrid sudden unaccounted load changes can cause variation in grid parameters. The primary level ensure that these variations are met and distributes it among the different ESS based on their characteristics. A frequency based splitting of the load will be done here.

The secondary level: It ensures that parameters (voltage, frequency etc) in the micro-grid are within the permissible range. The restoration to nominal values are achieved here.

The tertiary level The tertiary level forms supervisory level for the microgrid. This level ensures optimal power flow in the microgrid especially in islanded mode of operation. The optimal power flow problem decides the amount of power to be generated by the different sources so that some operational parameters are optimised. [7].

Central grid control unit This level supervises the operation of main grid . This level optimises main grid performance, decides which microgrid has to be connect to grid and energy exchange between different microgrids.

III. RESULTS

The initial work of the ESR focussed on the development of low level control for the power converters with emphasis on developing a reset controller for power converter. The improvement in the performance of the converter when catering to sudden load changes through minimisation of overshoot and faster settling time was highlighted in the previous works. Currently the ESR has developed a reset control based primary+secondary control scheme for a microgrid with hybrid storage system. The proposed architecture is shown in Fig.2. The control architecture was first developed under the assumption that the load data is known a priori. This assumption is reasonable as there will be higher levels in the real system which can estimate this value. The control architecture is basically made of three loops: the FC current control loop, the SC current control loop and voltage regulation loop. The objective here is to analyse the performance of the interconnected system when

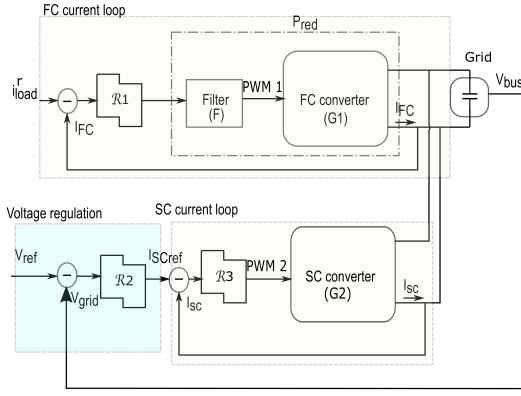


Fig. 2. Control architecture for the proposed system

the PI controller is replaced with the PI+CI controller. A simple rule for the power splitting is considered here. The FC converter will be provided with the load profile in the form of current reference (i_{load}^r) as shown in Fig.2. The FC control loop ensures that the reference value is followed. The FC control loop is designed slower than that of the SC control loop so that the FC does not meet the sudden load changes instantaneously but slowly ramp up and meet the reference value. The SC control loop is part of a multi-loop architecture. The outer loop is a voltage control loop which is tasked with maintaining the grid voltage (V_{bus}) at the nominal value thus regulating the DC bus voltage. The inner loop is the current loop which works on the reference from outer loop such that sufficient current is injected into the grid to ensure the grid voltage remain within prescribed range. Employing such a control architecture for the SC ensures that when the demanded load level changes the voltage difference created by the load imbalance as the FC ramps up in power will activate the SC outer loop causing the SC to supply the deficient power. Through this, sudden changes in load requirement will be met by the SC and larger imbalances by FC.

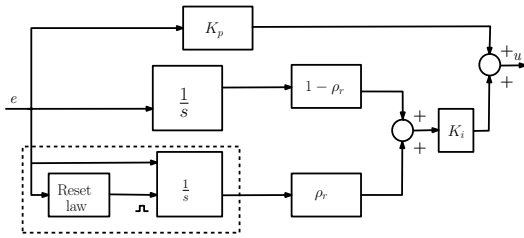


Fig. 3. Schematic of PI+CI controller

The design of parameters for the PI+CI controller shown in Fig.3 used in the control loops (shown as \mathcal{R} in Fig.2) like the proportional, integral gains and the reset ratio (ρ_r) is done as highlighted in the previous reports of the ESR. The comparison of PI+CI controller based voltage regulation control and PI based control is presented next. The Fig.4 shows current drawn from the grid under varying load profile (top) and the comparison of the DC grid voltage profile under

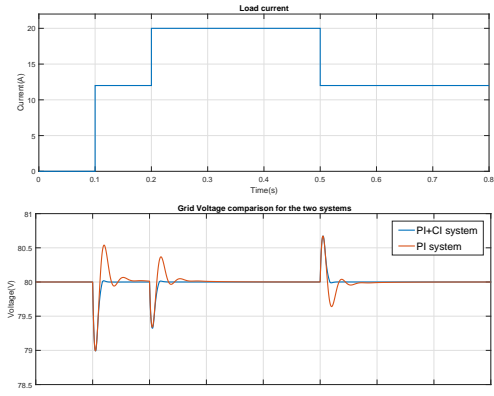


Fig. 4. The load profile introduced to DC grid (top) and comparison of grid voltages for PI+CI and PI based system under load variation (bottom).

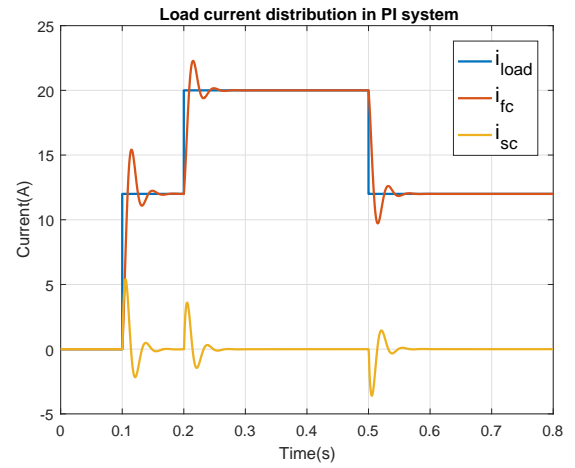


Fig. 5. Load current distribution among The FC and SC for the PI based system

the load variation for a system employing a PI+CI controller and PI controller (bottom). It can be noticed from Fig.4 that when the load variation is introduced in both systems there is a deviation in grid voltage until the first instance of zero error (nominal value). After this the reset action introduced by the reset controller of the voltage regulating loop ensures that grid voltage remains at the nominal value bringing the system controlled by PI+CI controller into steady state. In comparison the PI based systems as can be seen in Fig.4 takes a longer time to settle with more ringing in the grid voltage. This represents a clear improvement in voltage regulation performance achieved by reset PI+CI controller.

The Fig.5,6 represent the distribution of load current among the different ESS for system with PI and PI+CI controller respectively. The FC delivers major portion of the load current in both cases and the SC supplies the demanded load current when the FC ramps up in power. It can be seen from the comparison in Fig.5 and 6 that the overshoot in the current delivered by the FC and SC converters are avoided using the PI+CI controller. The flat response achieved by the reset controller is clearly visible in Fig.6.

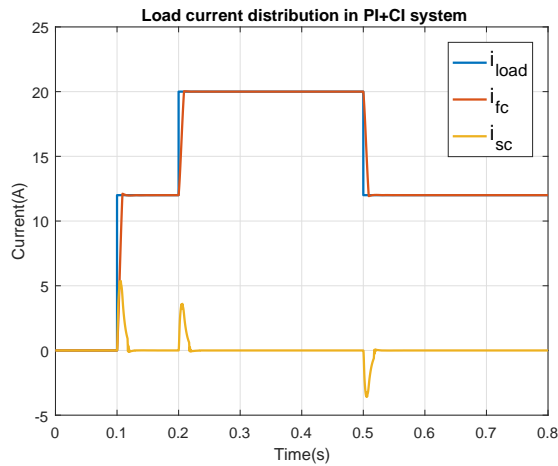


Fig. 6. Load current distribution among The FC and SC for the PI+CI based system

IV. RESEARCH STATUS

Presently the work done by the ESR is focussing on the development of an observer based control scheme for the estimation of the load demand in the grid based on the grid voltage profile. This scheme will be aided by a tertiary control scheme that will be developed to ensure optimal distribution of power among different sources. The proposed tertiary scheme will work on predicted voltage and load profiles to provide an optimal power distribution set points for the different storage units. The optimisation algorithm will be designed to minimise the rate of degradation of the different storage systems.

V. ACKNOWLEDGMENTS

This work is done as part of project which has received funding from the European Unions Horizon 2020 research and innovation programme under the Marie Skłodowska Curie grant agreement No 675318 (INCITE).

REFERENCES

- [1] Raphael Edinger and Sanjay Kaul. Humankind's detour toward sustainability: Past, present, and future of renewable energies and electric power generation. *Renewable and Sustainable Energy Reviews*, 4(3):295313, 2000.
- [2] Ali Ipakchi and Farrokh Albuyeh. Grid of the future. *IEEE Power and Energy Magazine*, 7(2):5262, 2009.
- [3] M S Dresselhaus and I L Thomas. Alternative energy technologies. *Nature*, 414(6861):3327, 2001.
- [4] Thomas Ackermann, Goran Andersson, and Lennart Soder. Distributed generation: A definition. *Electric Power Systems Research*, 57(3):195204, 2001.
- [5] Ibrahim, H., Ilinca, A., and Perron, J. (2008). Energy storage systems- Characteristics and comparisons. *Renewable and Sustainable Energy Reviews*, 12(5), 12211250. <https://doi.org/10.1016/j.rser.2007.01.023>
- [6] Chen, H., Cong, T. N., Yang, W., Tan, C., Li, Y., and Ding, Y. (2009). Progress in electrical energy storage system: A critical review. *Progress in Natural Science*, 19(3), 291312. <https://doi.org/10.1016/j.pnsc.2008.07.014>
- [7] Guerrero, J. M., Vasquez, J. C., Matas, J., De Vicua, L. G., and Castilla, M. (2011). Hierarchical control of droop-controlled AC and DC microgrids - A general approach toward standardization. *IEEE Transactions on Industrial Electronics*, 58(1), 158172. <https://doi.org/10.1109/TIE.2010.2066534>

Model Predictive Control Methods for Microgrids

ESR: Tomás Manuel Pippia
Supervisors: Bart De Schutter, Joris Sijs

I. INTRODUCTION

The concept of microgrids has been recently studied in the scientific literature due to the benefits that this architecture offers [1]–[3]. Microgrids can improve reliability, reduce the carbon emissions, and provide economic operation by reducing transmission and distribution costs [3]. Microgrids can also provide economical benefits because, by using information on predictions of renewable energy profiles and loads and on time-varying prices, a control strategy can be designed such that it provides optimal inputs that minimize an economical cost. In this regard, some works have proposed different Model Predictive Control (MPC) approaches for optimal operation of microgrids, e.g. [4]–[7]. The microgrid is modelled as Mixed Logical Dynamical (MLD) system [8], which means that the model includes both continuous and binary variables. Applying an MPC scheme to an MLD system yields a Mixed Integer Linear Programming (MILP) problem. This kind of problems can be solved by branch and bound solvers, but the problem has in general an exponential computational complexity. One way to mitigate this could be to parametrize the inputs in the model as in [9], such that the parameters of the control law, and not the control inputs, are optimized. A reduction in computational complexity can be achieved if the number of parameters is less than the number of inputs. Another possible solution could be to combine MPC with some heuristic or rule-based rules, in order to improve the speed of the optimization procedure. In this abstract, we present two different MPC methods for an energy management system of microgrids. The first method expresses the inputs as a function of the parameters and other variables; the second method assigns the values to the binary variables in the MLD model and reduces the optimization problem to a linear programming one.

II. MODELING

We follow the modeling approach from [4]. Variables related to the microgrid are described using an MLD modeling framework. The states of the model represent the level of charge in the energy storage system and their dynamics are

$$x_b(k+1) = x_b(k) + T_s \left(\eta_{c,b} - \frac{1}{\eta_{d,b}} \right) z_b(k) + \frac{T_s}{\eta_{d,b}} P_b(k),$$

where x_b represents the level of charge of the battery, T_s is the sampling time, $\eta_{c,b}, \eta_{d,b}$ represent the charging and discharging efficiencies, respectively, P_b is the power exchanged with the energy storage system, z_b is an auxiliary variable used in the MLD model, and k is the current time

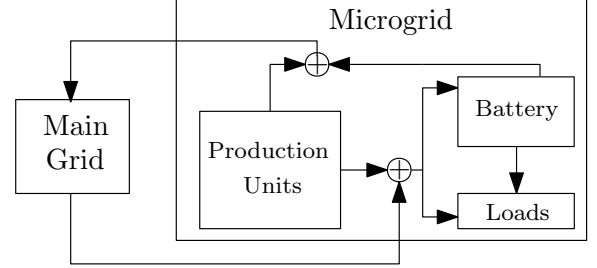


Fig. 1. Microgrid scheme considered for our work. Arrows represent power flows.

step. The system is subject to many constraints, e.g. lower and upper bound constraints, generator constraints. However, the most important constraint is given by the internal power balance of the microgrid:

$$P_b(k) = \sum_{i=1}^{N_g} P_i^p(k) + P_{res}(k) + P_{grid}(k) - P_{load}(k), \quad (1)$$

where P_i^p is the power produced by the local dispatchable generator i , $i \in \{1, \dots, N_g\}$ with N_g the total number of dispatchable generators, P_{res} the power produced by the local renewable energy sources, P_{load} the local power demand, and P_{grid} the power exchanged with the main grid. Constraint (1) has to be satisfied at all times. Note also that in (1) we express P_b as a function of all the other variables, thus (1) can be used to eliminate P_b from the optimization problem within the MPC problem. Therefore, the it is possible to optimize only P_{grid} and P_i^p , $i \in \{1, \dots, N_g\}$.

We also consider time-varying electricity prices, such that prices for purchase and sale of electricity are different. We denote with c_{sale} and c_{pur} the price for selling and purchasing electricity to and from the main grid, respectively. We also consider a fixed tariff c_{prod} for producing electricity with the local production units.

III. PARAMETRIZATION OF CONTROL INPUTS

In the first approach that we propose, the control inputs are parametrized as a function of parameters and other quantities such as the electricity prices, inspired by [9]. The idea is to express the inputs as a combination of different terms that are weighted by some parameters. The two control inputs to be optimized are P_{grid} and P_i^p and they are parametrized as

$$P_{grid}(k) = -\theta_1 c_{pur}(k) - \theta_2 c_{sale}(k) + \theta_3 f_{bal}(k-1) \quad (2)$$

$$P_i^p(k) = \theta_4 P_{load}(k) + \theta_5 c_{pur}(k) + \theta_6 (\bar{x}_b - x_b(k)) \quad (3)$$

where $f_{\text{bal}}(k-1) = -P_{\text{load}}(k-1) + P_{\text{res}}(k-1) + \sum_{i=1}^{N_g} P_i^{\text{P}}(k-1)$ represents the local power balance between production and consumption at the previous time step and \bar{x}_b is the maximum energy storage level of the battery. The idea behind the parametrization (2)-(3) is to have different terms that are weighted by the parameters θ_1 - θ_6 . The objectives in (2) are defined in such a way that less power is imported from the grid if the purchase price or the sale price is high, while more power is imported if at the previous time step the microgrid was not able to satisfy the local loads with its internal power production resources, i.e. renewable energy sources and dispatchable generators. The objectives in (3) are similar: more power is produced locally when the loads are high, when the price for importing electricity is high, and when the battery has a low storage level.

Note also that the parameters θ_1 - θ_6 are not time-varying. This means that the same parameters are used for the whole prediction horizon and therefore, in this case, we have only 6 optimization variables. This can provide computational savings if the number of inputs is higher than 6, which is translated into a prediction horizon larger than 3, since we have two control inputs in this case.

IV. IF-THEN-ELSE RULES FOR THE BINARY DECISION VARIABLES

In this second method, we follow a completely different approach. Instead of parameterizing the inputs as a function of the parameters, we assign the value to the binary decision variables in the MLD model by following if-then-else rules. Then, after all the binary variables have been assigned, the optimization problem is transformed from an MILP problem to a linear programming one, yielding great computational savings.

The if-then-else ruling is based on two main questions: is $P_{\text{res}}(k) \geq P_{\text{load}}(k)$? Is $c_{\text{prod}}(k) < c_{\text{sale}}(k) < c_{\text{pur}}(k)$ or $c_{\text{sale}}(k) < c_{\text{prod}}(k) < c_{\text{pur}}(k)$, or $c_{\text{sale}}(k) < c_{\text{pur}}(k) < c_{\text{prod}}(k)$? Based on the answer to these questions, the controller makes different decisions and assigns the values to the binary variables in the MLD model.

We show now an example of how the if-then-else rules work. Suppose that $P_{\text{res}}(k) < P_{\text{load}}(k)$ and that $c_{\text{prod}}(k) < c_{\text{sale}}(k) < c_{\text{pur}}(k)$. In this case, the renewable energy sources are not able to completely satisfy the local loads, thus the local net imbalance is negative. Energy has to be produced locally, and since the production price of electricity is smaller than the purchase price, we turn on the dispatchable units. We allow the extra power produced by these units to be sold to the main grid, or to be stored in the battery. If, instead, we had $c_{\text{sale}}(k) < c_{\text{pur}}(k) < c_{\text{prod}}(k)$, it would be more expensive to produce electricity locally rather than buying it, and then the production units would be turned off and we would set the power exchange with the grid to the import mode. Moreover, in order to reduce the cost, the battery would be allowed to provide some of the stored energy.

Based on this if-then-else rules, the unit commitment problem and the problem of choosing the mode of operation of the battery, i.e. charge or discharge, and of the power

exchange with the main grid, i.e. import or export, are solved by the if-then-else rules. Then, during the MPC optimization procedure, a linear programming problem is solved, which is much faster than an MILP. The optimization variables in these case are again P_{grid} and P_i^{P} , $i \in \{1, \dots, N_g\}$.

V. CONCLUSIONS

We have presented two different MPC methods for optimal operation of microgrids. In the first method, we express the control input as a function of the parameters and other variables, while in the second method we assign the value to the binary decision variables through an if-then-else ruling. Both methods reduce the computational complexity, since they either reduce the number of optimization variables or they convert a MILP problem into a linear programming one.

A thorough comparison of the proposed methods opposed to the standard approaches in the literature will be carried out to assess the benefits of our approaches.

ACKNOWLEDGMENTS

This project has received funding from the European Unions Horizon 2020 research and innovation programme under the Marie Skłodowska-Curie grant agreement No 675318 (INCITE).

REFERENCES

- [1] X. Fang, S. Misra, G. Xue, and D. Yang. Smart grid — the new and improved power grid: A survey. *IEEE Communications Surveys Tutorials*, 14(4):944–980, 2012.
- [2] N. Hatziaargyriou, H. Asano, R. Iravani, and C. Marnay. Microgrids. *IEEE Power and Energy Magazine*, 5(4):78–94, 2007.
- [3] S. Parhizi, H. Lotfi, A. Khodaei, and S. Bahramirad. State of the art in research on microgrids: A review. *IEEE Access*, 3:890–925, 2015.
- [4] A. Parisio, E. Rikos, and L. Glielmo. A model predictive control approach to microgrid operation optimization. *IEEE Transactions on Control Systems Technology*, 22(5):1813–1827, 2014.
- [5] S. Raimondi Cominesi, M. Farina, L. Giulioni, B. Picasso, and R. Scattolini. A two-layer stochastic model predictive control scheme for microgrids. *IEEE Transactions on Control Systems Technology*, 26(1):1–13, 2018.
- [6] F. Kennel, D. Görges, and S. Liu. Energy management for smart grids with electric vehicles based on hierarchical MPC. *IEEE Transactions on Industrial Informatics*, 9(3):1528–1537, 2013.
- [7] J. Sachs and O. Sawodny. A two-stage model predictive control strategy for economic diesel-PV-battery island microgrid operation in rural areas. *IEEE Transactions on Sustainable Energy*, 7(3):903–913, 2016.
- [8] A. Bemporad and M. Morari. Control of systems integrating logic, dynamics, and constraints. *Automatica*, 35(3):407–427, 1999.
- [9] S. K. Zegeye, B. De Schutter, J. Hellendoorn, E. A. Breunese, and A. Hegyi. A predictive traffic controller for sustainable mobility using parameterized control policies. *IEEE Transactions on Intelligent Transportation Systems*, 13(3):1420–1429, 2012.

A Statistical Physics Approach to Dynamic Coherency (or lack of) in Large HVDC Grids

Adedotun J. Agbemuko
and José Luis Domínguez-García
Department of Electrical Power Systems
Institut de Recerca en Energia de Catalunya (IREC)
Barcelona, Spain.
Email: aagbemuko@irec.cat

Oriol Gomis-Bellmunt
Department of Electrical Engineering
Universitat Politècnica de Catalunya
Barcelona, Spain.

Abstract—This paper studies the coherency of large-scale HVDC networks from a theoretical perspective based on a statistical physics approach. A theoretical analysis of twelve terminal, 18 cable HVDC network is carried out.

Index Terms—Coherency, networked systems, statistical physics

I. INTRODUCTION

The increasing penetration of renewable energy sources (RESs) and emerging technologies has meant that power electronic converters are becoming the fundamental building blocks of future networks. A general consensus in power systems is the expected role of power electronic converters and DC circuits. Particularly, it is expected that a DC grid would share a similar responsibility as the existing AC grid or even take on the entire responsibility. This is expected to bring in an entirely new dynamics on the system. Therefore, more effort is needed in extensively understanding the DC grid.

It is widely expected that into the future, multi-terminal high voltage DC (HVDC) circuits and systems would emerge from the current HVDC link structure. Therefore, it is important to understand the impact of topological properties and aggregate behaviour of large-scale HVDC networks. From the perspective of the conventional AC grid, the research community have applied the concept of coupled oscillators to understanding the oscillatory behaviour of synchronous generators connected over large networks. Especially the impact of topological features, network, control, and overall coherency of the system [1]–[4]. However, it does not suffice to directly extend such coupled oscillator behaviour to DC grids as power converters are not natural oscillators. Besides, the DC network is reasonably linear in comparison to the AC grid. However, coherency of responses, for instance, voltage responses could be studied to understand the impact of topological features and control on such responses.

Literature on the study of coherency for DC grids is almost non-existent. Coherency implies the ability of responses to stay within defined bounds in steady-state or during dynamic

responses. In a similar vein, it is interesting to observe the overall aggregate response of the DC grid for random variations in system parameters such as, topology, operating point, and control systems.

In this paper, we aim study the dynamic coherency of meshed HVDC grids without any form of control as a first step. In this manner we can observe the natural behaviour and aggregate response of the DC network over time in addition to another variable herein referred to as the control parameter.

II. METHODOLOGY FOR COHERENCY STUDY IN HVDC GRIDS

There are several approaches to tackle the problem at hand. The final aim is to understand how to bring the system from one state to another, and how fast this can be done. In this work, a statistical physics approach is presented and the focus is on dynamics during disturbances and changes in the system. Therefore, time plays a major role as opposed to in steady-state where theoretically, time plays little or no role.

The statistical physics approach followed is often referred to as *order parameter analysis*. Such method allows to obtain insights into how the system transitions from one ‘phase’ to another if there are any. Therefore, we need to observe the natural transition in order to determine how control should keep system in coherency state for as long as possible. It is important to make clear at this juncture that this paper is from a purely theoretical perspective and several concepts might appear counter-intuitive from a practical point of view. Justifications and clarifications would be made as necessary to balance theory and application.

A. Order Parameter Analysis

This is a statistically dependent analysis where a set control parameter (or external disturbance parameter) is generated relative to the network impedances (or admittance) which is a measure of strength of coupling. For instance, a *zero* impedance (or infinite admittance) implies complete order from a theoretical view. Whereas, an infinite impedance implies complete disorder. It is important to note that infinite in this work is relative from the perspective of impedances. For instance, infinite impedance could refer to the impedance of

This work was financially supported by the European Union’s Horizon 2020 research and innovation programme under Marie-Sklodowska-Curie action INCITE – “Innovative controls for renewable source integration into smart energy systems”, grant agreement No. 675318.

a 20,000 km cable, which is too high to be practical, hence, infinite. An infinite impedance could also refer to a material of very high resistance compared, whereas *zero* impedance could refer to a super-conducting material with relatively low impedance. The former example is intuitive as the analysis in this work is based on scaled impedances between 0 – 1 with 1 as infinite impedance. Therefore, practical impedances and that of a realistic system will be in the range 0.001 – 0.05.

The method of order parameter depends mainly on generating an R_f random sets of cable resistances. Where a random set is a vector of dimension $1 \times n_c$ and n_c is the number of cables in the system. Thus, for R_f random sets of a 3 cable network, the total dimension of random resistances is a $R_f \times 3$ matrix, R_m . Subsequently, a deterministic vector T_0 of values between 0 – 1 of any size k (for example, k equally spaced values) is generated; this is the vector of control parameter. Subsequently, each element in R_m is compared with each element of T_0 , the control parameter and a rule applied to obtain a new R_m , referred to as R_m^p such that, if

$$\begin{aligned} R_m(i, j) &> T_0(k) \quad \forall \quad i, j \in (R_f \times n_c) \\ R_m(i, j) &= T_0(k) \end{aligned} \quad (1)$$

that is, any random resistance with a value greater than the chosen element of T_0 is replaced by the chosen value of T_0 . This is done for all $T_0(k)$, resulting to a 3-D matrix (R_m^p) of dimension, $R_f \times n_c \times k$.

Subsequently, the system dynamic equations given in (2) is solved for each set of n_c resistances in the 3-D matrix. That is, the time-domain solution solved for $R_f \times n_c \times k$ system. For a large HVDC grid, of say fifteen cables and twelve terminals translates to significant computational requirements depending on the time steps of solver.

$$\dot{\mathbf{V}} = -\text{diag}(1/C_1, \dots, 1/C_n) \mathbf{Y}_{bus} \mathbf{V} + \text{diag}(1/C_1, \dots, 1/C_n) \mathbf{I} \quad (2)$$

where \mathbf{V} is the vector of terminal voltages, \mathbf{I} is the vector of current injection, and C_1, \dots, C_n are the terminal capacitances.

III. PRELIMINARY STUDIES ON A LARGE HVDC GRID

In this section the uncontrolled dynamics of the HVDC depicted in Fig. 1 based mainly on terminal capacitance is modelled and equation (2) is for each set of random system in the 3-D matrix R_m^p . Without applying the order parameter and solving the HVDC equations for the physical system. Fig. 2 shows the theoretical response (natural dynamics) of the HVDC grid for a balanced power flow with the same initial conditions at all terminals.

REFERENCES

- [1] F. D. “Synchronization in complex networks of phase oscillators: A survey,” *Automatica*, vol. 50, no. 6, pp. 1539 – 1564, 2014. [Online]. Available: <http://www.sciencedirect.com/science/article/pii/S0005109814001423>
- [2] J. W. Simpson-Porco and F. D. “Synchronization and power sharing for droop-controlled inverters in islanded microgrids,” *Automatica*, vol. 49, no. 9, pp. 2603 – 2611, 2013. [Online]. Available: <http://www.sciencedirect.com/science/article/pii/S0005109813002884>

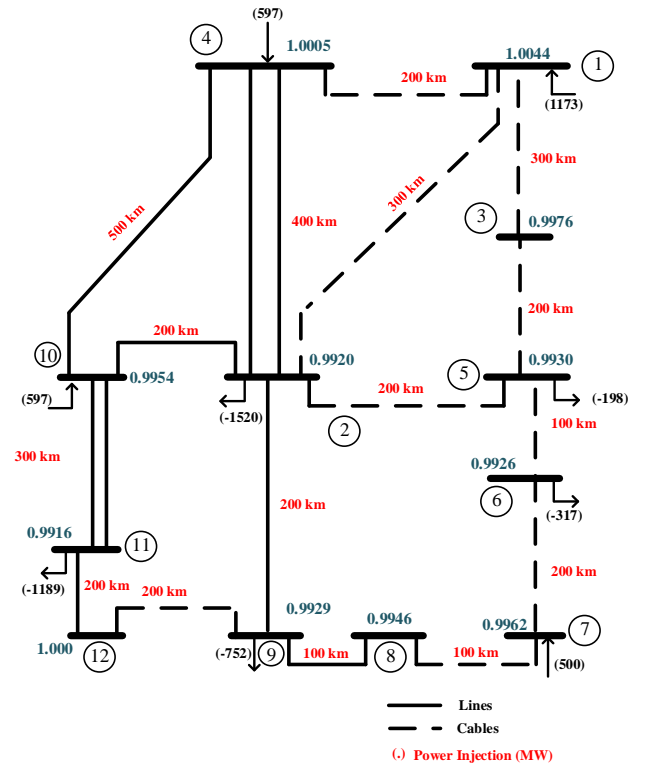


Fig. 1. Cigré HVdc Grid

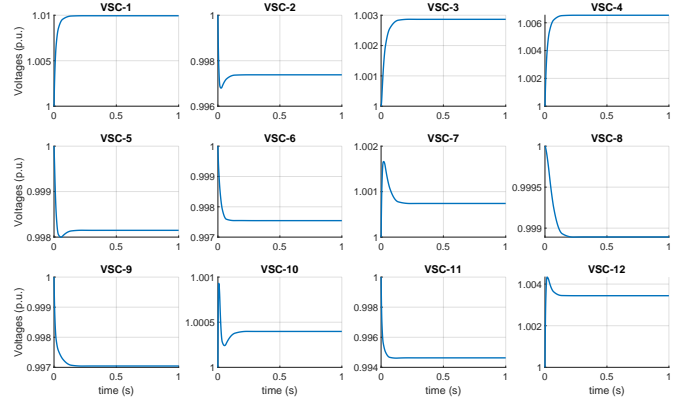


Fig. 2. Theoretical Responses of Uncontrolled HVDC Grid

- [3] T. Nishikawa and A. E. Motter, “Comparative analysis of existing models for power-grid synchronization,” *New Journal of Physics*, vol. 17, no. 1, p. 015012, 2015.
- [4] F. Dörfler and F. Bullo, “On the critical coupling for kuramoto oscillators,” *SIAM Journal on Applied Dynamical Systems*, vol. 10, no. 3, pp. 1070–1099, 2011. [Online]. Available: <https://doi.org/10.1137/10081530X>

INCITE Workshop Jul 2018 - Deliverable 6.5

IRP32: A new modeling approach for stabilization of smart grids

Felix Koeth

Abstract—Offshore wind parks are a promising technology for renewable energies. Ideally, this parks would be connected to the main grid using HVDC connections, which reduces line losses. The converters necessary to connect wind farm with the AC-System can lead to instabilities in the power system, due to the loss of inertia. This work shows how a control scheme for the offshore converters can lead to a inertia support of the AC-System.

I. INTRODUCTION

The transition to renewable energies is a crucial task in technology. Renewable energies are vital to combat climate change, but also reduce the dependency on natural resources. One major concern is the stability of the electrical grid, which is challenged by the change in the topology of the network, the introduction of new dissimilarity in the network and the usage of new electric devices, which will reduce the inertia and damping of the system. For many European countries, wind energy is one of the most promising renewable energy source. One very popular option, especially in the North Sea are offshore wind parks, which benefit from the steady wind conditions on the open sea while being less obstructive on land. Big offshore wind parks with a capacity over 600 MW are already installed and in operation. A major problem is the transportation of the energy to the main land. To reduce line losses due to high resistance in long distance lines, a HVDC link might be desirable. To make use of a HVDC line, the current has to be converted twice, offshore (from the AC current generated by the wind park and onshore, to inject the current in the main AC grid. Two major challenges arise on the conversion:

- The power electronics used in the converters don't add inertia to the grid
- The controllability of the wind park has to be taken to account

In this paper, the work from [1], which incorporates a novel control method which aims to overcome this issues is presented and investigated.

II. MODELING BACKGROUND

A typical system which is supposed to be analyzed is shown in Figure 1. The two AC-Systems A and B and a wind farm are connected by a 4 terminal DC grid. This system was introduced in [1]. The main goal of this study is to investigate how the converters and the wind farm influence the frequency deviations Δf_i of the Systems (A and B).

Felix Koeth is with G2Elab, University of Grenoble, 38031 Grenoble, France felix.koeth@g2elab.grenoble-inp.fr

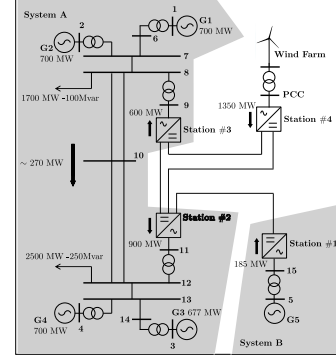


Fig. 1. Example network featuring onshore grids and an offshore wind park.

For that, we need to incorporate control strategies for the converters and the wind park and model the dynamics of the main AC-Systems.

A. Onshore converters

The onshore converters are controlled using a classical droop controllers. Here, a $P-V$ droop is recommended which allows the operation of the HVDC voltage control mode. A $f-V$ droop control scheme is also included in the converter. This allows frequency support between connected AC-Systems and the inertial response of the HVDC link. The mathematical formulation, using the droop control parameters k_f and k_p is given as:

$$V_{dc} = V_{dc}^{ref} - k_p (P_{dc} - P_{dc}^{ref}) + k_f (f - f^{ref}) \quad (1)$$

B. Offshore converters

The main idea in this study is to use a communication based control strategy for the offshore converters. Using fiber-optic cables, the frequencies of the onshore systems is communicated to the offshore converters. Using this information, the wind parks can react to frequency deviations of the onshore systems and provide inertial support. Mathematically, the offshore frequencies f^{off} are calculated from the frequencies of the n_{on} onshore converters using a weight term g_j as:

$$f^{off} = f^{ref} + \sum_{j=1}^{n_{on}} g_j (f_j - f_j^{ref}) \quad (2)$$

C. Wind farm

The wind park can provide frequency support by changing the rotor speed of the blades. Here, the inertial response for

the wind turbines is given by using modification of the power by the derivative of the frequency variations given as:

$$\Delta P = -K_I \frac{d\Delta f}{dt} \quad (3)$$

D. Swing equation

Using the swing equation and the fact that the power exchange of the HVDC grid is zero, the following incorporated model for frequency deviations of the onshore systems i can be calculated as:

$$H'_i \frac{d\Delta f_i}{dt} - D'_i \Delta f_i = -\tilde{P}_i^{ref} + \underbrace{\sum_{k \neq i}^N \left(A_{ik} \Delta f_k + B_{ik} \frac{d\Delta f_k}{dt} \right)}_{Q_{ik}} \quad (4)$$

The augmented inertia here is given as $H'_i = 2H_i + \beta_i n_{off} K_I \sum_j^{m_i} g_j$. Thus, the control scheme will increase the total inertia of the AC-Systems, improving on the problem of the low inertia in power systems with an HVDC grid. The term Q_{ik} indicates the coupling between the AC-Grids i and k . As frequency droop controllers are used as converters, the AC-Systems feel a frequency response from the other systems.

III. ANALYSIS

The resulting mathematical model (4) can be analyzed theoretically. In [1], it was incorporated in a realistic generator model. The model can also be investigated without any generator model. In vector form, the system is given as:

$$(H' - B) \frac{d\Delta f}{dt} = -P + (A - D') \Delta f \quad (5)$$

The behavior of the frequency deviations can thus be calculated by the eigenvalues of the matrix $(H' - B)^{-1}(A - D')$. Using the system given in [1], the eigenvalues of the matrix are always negative, so frequency variations around the reference frequency will decline. For general systems ($N > 3$), positive eigenvalues were observed.

IV. OUTLOOK

The current framework focuses on the influence of the offshore links. The behavior of the AC-Systems is ignored. Possibility to model droop controllers in a simplified power system model is given in [2], [3], where it was shown that droop controllers in an AC-System behave like Kuramoto oscillators. A future step would be to incorporate the converter modeling of the offshore converters to this approach and model the AC-System not as a single system, but a network of generators and loads. While the general stability properties of the AC-System ([4], [5]) should not be affected by the droop controller with constant power, the modeling of the HVCD network and the wind farm will influence the dynamics of the network. For the model introduced here, precise conditions for the stability or instability would be of interest. For that, the properties of the matrices have to be investigated in detail and parameter ranges for the involved

parameters have to be found. General questions about how to use general, simplified control schemes and their interaction with complex power systems is still ongoing. While the damping term in the swing equation already provides a frequency regulation, a more complex control scheme, like the one introduced here might be interesting.

V. ACKNOWLEDGMENTS

This project has received funding from the European union's Horizon 2020 research and innovation programme under Marie Skłodowska-Curie grant agreement No 675318

REFERENCES

- [1] I. Martínez Sanz, B. Chaudhuri, and G. Strbac. Inertial Response From Offshore Wind Farms Connected Through DC Grids. 30(3):1518–1527.
- [2] John W. Simpson-Porco, Florian Dörfler, and Francesco Bullo. Synchronization and power sharing for droop-controlled inverters in islanded microgrids. 49(9):2603–2611.
- [3] John W. Simpson-Porco, Florian Dörfler, and Francesco Bullo. Droop-Controlled Inverters are Kuramoto Oscillators*. 45(26):264–269.
- [4] Florian Dörfler and Francesco Bullo. Synchronization in complex networks of phase oscillators: A survey. 50(6):1539–1564.
- [5] Francisco A. Rodrigues, Thomas K. DM. Peron, Peng Ji, and Jürgen Kurths. The Kuramoto model in complex networks. 610:1–98.

Wind farms control strategies for grid support

Sara Siniscalchi-Minna, Mikel De-Prada-Gil and Carlos Ocampo-Martinez

I. INTRODUCTION

Wind farm control strategies are commonly focused on maximizing total energy yield or increasing the lifetime of wind turbines though mechanical load reduction. Additionally to the previously mentioned objectives, wind farms are more frequently asked to participate in ancillary services, so far relied on conventional power plants, due to the increasingly wind energy penetration level into the electrical grid [1]. Wind turbines do not inherently provide these services, but advanced control strategies have been proposed for wind farms and wind turbines to regulate both active and reactive power in order to contribute to power system stability by providing support for grid voltage and frequency. For example, it is required for wind farms to participate in frequency control providing the power balance after frequency deviations. In Figure 1, it is shown the effect of including non-synchronous generators, such as wind turbines, in an electrical grid previously dominated by synchronous generators and the improvement achieved providing frequency support with wind farms. Conventionally, grid frequency response is divided into separate control regimes: inertial, primary and secondary responses. The wind turbines can take part in inertial frequency support releasing, within milliseconds, the kinetic energy stored in the rotating mass during the normal operation. Likewise, in case of high wind energy generation, wind farms can also participate in primary frequency control delivering extra active power, (i.e. the power reserve) within seconds by operating in de-loading mode. Thus, wind farms can meet the grid requirements and generate less power than the maximum available to guarantee the demand. This work focuses on increasing the power reserve that can be delivered into the grid whilst accomplishing the TSO requirements. Previous works have shown that this objective can be achieved by redirecting the flow around downstream turbines applying either induction or yaw control. Several computational fluid dynamics simulations and wind tunnel experiments have shown that those methods can increase power without substantially increasing turbine loads [2]–[4]. The most common approach is to use

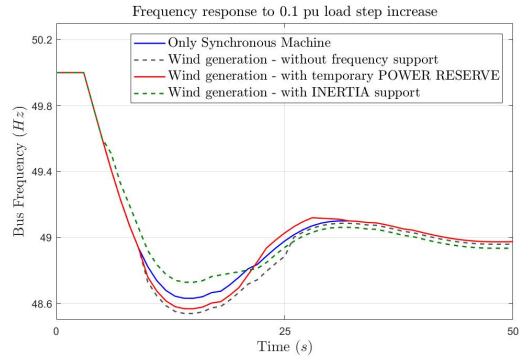


Fig. 1. Frequency drop and wind energy frequency support.

a centralized control strategy but however this breaks down when the individual turbines are unavailable. Additionally in large wind farms the high number of information sharing between the turbines and the central controller could reduce the performance for on-line optimization. To cope with this issue, a decentralized optimization framework is proposed in this work to enable real-time optimization, which is much more difficult to achieve using centralized techniques. This work demonstrates that a wind farm can be modeled as a distributed system by partitioning it into subsets according to wake interactions.

II. DECENTRALIZED CONTROL STRATEGY

A wind farm can be represented as a directed network, wherein each turbine represents a node in the network and the aerodynamic interactions between turbines due to the wake effect can be represented as edges of this directed network [5]. The wind farm is a directed network because actions of the upstream turbines affect the downstream turbines, but downstream turbine actions do not affect upstream turbines. For the wind farm problem, the strength of each edge is assigned based on the strength of the wake impacting the downstream turbine (see Figure 2). The strength between an upstream turbine i and the downstream turbine j is determined by: distance downstream x_{ij} , area overlapped $A_{s,i}$ based on thresholding, and wind turbine characteristic r_0, r_i, A_0 [6]. The edge strengths are defined as:

$$\epsilon_{ij}(\phi) = \left| \frac{r_0}{r_i(x_{ij})} \right| \frac{A_{s,i}(\phi)}{A_0}, \quad (1)$$

Based on these strengths, a wind farm can be divided into subsets. The partitioning problem is stated to find the optimal set of partitions such that the following objectives are ensured: 1) Minimize the edges between different par-

S. Siniscalchi Minna and M. De Prada Gil are with Catalonia Institute for Energy Research, IREC, Jardins de le Dones de Negre, 08930 Sant Adri de Bess, Barcelona (Spain). {ssiniscalchi,mdprada}@irec.cat

S. Siniscalchi-Minna and C. Ocampo-Martinez are with the Automatic Control Department, Universitat Politècnica de Catalunya, Institut de Robòtica i Informàtica Industrial (CSIC-UPC), Llorens i Artigas, 4-6, 08028 Barcelona, Spain. {ssiniscalchi,cocampo}@iri.upc.edu

This work has received funding from the European Union's Horizon 2020 research and innovation programme under the Marie Skłodowska-Curie grant agreement No 675318 (INCITE).

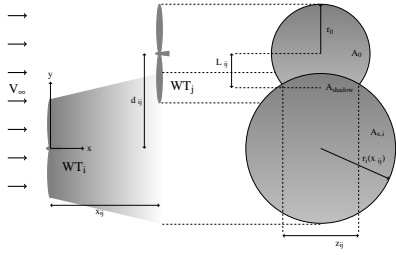


Fig. 2. Wake expansion.

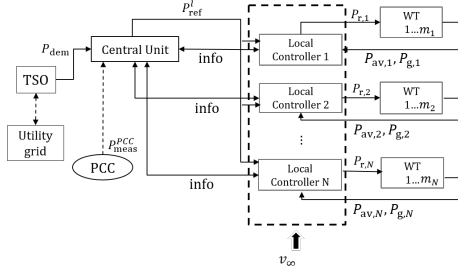


Fig. 3. Wind farm hierarchical control scheme.

titions. This objective may be ensured maximizing the couplings among the turbines caused by the wake propagations. 2) Minimize the distance among the turbines belonging to the same partition. This objective is added to ensure unique solution when no wakes affect the downstream turbines. 3) Minimize the difference between the amount of turbines in the partitions. The aforementioned objectives are hierarchically prioritized to find the optimal partition by solving a mixed-integer multi-objective optimization problem. Meanwhile, the proper number of subsets is evaluated according to the wind farm layout and the dominant free-stream speed direction such that the turbines affected by the same wake effect are included in the same partition.

Control Scheme: The hierarchical wind farm decentralized control scheme is shown in Figure 3. The wind farm control operates at two-time scales. According to the variation of the dominant free-stream wind speed in the time-frame of several minutes, the optimal partitions are updated, while the active power control acts within seconds in order to ensure the grid requirements. In fact, a central unit receives the power demand profile P_{dem} required by the TSO and, according to the information exchange with the local controllers, which are available power in the partition P_{av}^l and power generated P_g^l for $l \in K$, computes the power references to be addressed to the local controllers P_{ref}^l . Hence, in order to generate the desired power, each controller sets the power set-points for the turbines within the partition $P_{r,i}, i \in V^l$ according to the available and generated powers of every single turbine. In this work, a de-loading active power control strategy is proposed to guarantee two objectives: 1) dynamically tracking the power demand profile required by the TSO, 2) regulating the power references for each partition and the power set-points for each turbine such that the power reserve of the wind farm is improved.

In order to reduce the power losses due to the wake effects, an heuristic power dispatch approach to distribute the power demanded by the grid among the partitions may be focused on prioritizing the power generation of those partitions that can provide more power, i.e., the partitions with low number of downstream turbines. Meanwhile, the power contribution of the partitions more affected by the wakes should be set to ensure de-loading operation. In order to ensure the aforementioned power dispatch approach, the controller in the central unit solves a linear programming problem presented in [2].

The main objectives of the local controller are: O1) Ensure the power reference sent by the central unit. O2) Distribute the power set-points among the turbines in order to maximize the available power (i.e. the power reserve) of each partition. In order to satisfy the aforementioned objectives, the model predictive control strategy presented in [7] is implemented for each local controller.

The proposed control strategy was evaluated for a wind farm with 30 benchmark NREL-5MW wind turbines. The results show that the mean value of power reserve obtained with the proposed approach results to be increased about 11,5% with respect to the centralized strategy.

III. ON-GOING WORK

Preliminary results have indicated that additional benefit can be obtained with distributed control strategy. In this case, the computational cost when compared to solving a fully centralized optimization can be reduced providing similar power gain results. Reducing the computational cost of the overall optimization problem allows for these wind farm control strategies to be deployed in real time. Moreover, in [3] it has been shown that the presented optimization-based control strategy can also minimize the electrical power losses in the electrical connections among the turbines; thus, an additional step of the present work is to compute both active and reactive power flows to evaluate such losses.

REFERENCES

- [1] WWEA, "WWEA half-year report: worldwind capacity reached 456 GW," Oct. 2016.
- [2] S. Siniscalchi Minna, F. Bianchi, M. De Prada Gil, and C. Ocampo Martinez, "A wind farm control strategy for power reserve maximization," *Renewable Energy Journal*, 2018.
- [3] S. Siniscalchi-Minna, M. De-Prada-Gil, F. Bianchi, C. Ocampo-Martinez, and B. De Schutter, "A multi-objective predictive control strategy for enhancing primary frequency support with wind farms," in *Journal of Physics: Conference Series*, vol. 1037, no. 3. IOP Publishing, 2018, p. 032034.
- [4] F. Campagnolo, V. Petrović, C. L. Bottasso, and A. Croce, "Wind tunnel testing of wake control strategies," in *American Control Conference*. IEEE, 2016, pp. 513–518.
- [5] J. Annoni, C. Bay, T. Taylor, L. Pao, P. Fleming, and K. Johnson, "Efficient optimization of large wind farms for real-time control," in *Proc. of American Control Conference (ACC)*, 2018, pp. 6201–6205.
- [6] S. Siniscalchi-Minna, F. Bianchi, M. De-Prada-Gil, C. Ocampo-Martinez, and B. De Schutter, "Partitioning approach for large wind farms: Active power control for optimizing power reserve," in *Proc. of American Control Conference (ACC)*, 2018, pp. 6201–6205.
- [7] S. Siniscalchi Minna, F. Bianchi, and C. Ocampo Martinez, "Predictive control of wind farms based on lexicographic minimizers for power reserve maximization," in *Proc. of American Control Conference (ACC)*. IEEE, 2018, pp. 701–706.

Multistage Stochastic Optimization Programming for the operation of Local Energy Systems

C. Orozco, A. Borghetti, S. Lilla, G. Pulazza, F. Tossani
Department of Electrical, Electronic and Information Engineering
University of Bologna, Italy

Abstract— The paper deals with the optimization of the operation of a local energy system consisting of photovoltaic units, energy storage systems and loads aimed at minimizing the electricity procurement cost. The paper describes the generation of the scenarios, the construction of the scenario tree and an alternative to the final scenario tree reduction. Moreover, an intraday decision-making procedure based on the solution of the multistage stochastic programming was introduced to perform the numerical tests, in order to evaluate the implemented approach. An extended version of the paper has been presented in [1]

Keywords—Energy scheduling; Local energy system; Mixed integer linear programming; Stochastic programming; Scenario reduction; Monte Carlo method; Kinetic Battery Model.

I. INTRODUCTION

The considered system includes a photovoltaic (PV) unit capable to provide a significant part of the local energy consumption and an energy storage unit to fully exploit the available renewable energy source even for the case of a limited capability of the external utility network to which the system is connected.

We focus here on the solution of the day-ahead scheduling, which is in general associated with a real time control of the integrated PV-storage system, as dealt with in e.g., [2],[3]. A typical aim of the energy management system is the minimization of the power exchange with the external network to feed the internal load in a time horizon T .

II. MULTISTAGE STOCHASTIC OPTIMIZATION PROCEDURE

We assume that both the load profile and the PV generation are uncertain, whilst, to limit the complexity of the model, the prices (in €/kWh) of the energy exchanged with the external grid are assumed known (p_t^{imp} and p_t^{exp} , bought and sell, respectively).

The decision variable is the battery power output P_t^b and the objective function is the minimization of the energy procurement costs. The decision is taken at the beginning of the day (which is the scheduling horizon) for all the periods of the first 6 hours and the decision is updated every 6 hours. The five moments when the decision is taken represent the stages of the problem. The values of the other variables are calculated at the end of each 6 hour periods.

The five-stage stochastic optimization problem needs a scenario tree model that is built by using the k -means clustering method.

In the following, we describe the procedures adopted for the generation of set of initial scenarios Ω , for the construction of the scenario tree that is used in the recourse model, and the intraday decision-making procedure that uses both the day-ahead solution of the multistage stochastic problem and the knowledge of the actual PV generation and load request.

A. Generation of scenarios

For the scenario generation, we have applied the procedure described in e.g. [4], which includes a Markov-process to represent the autocorrelation that exists between consecutive observations. Starting from the forecasted profiles P_t^{pv} and P_t^{load} , at first they are normalized by using the corresponding mean value and standard deviation; then, for each scenario ω , the normalized time series y_t^{pv} and y_t^{load} are given by

$$\begin{aligned} z_{\omega,t} &= x_{\omega,t} + y_t \\ x_{\omega,t} &= \phi \cdot x_{\omega,t-1} + \varepsilon_{\omega,t} \end{aligned} \quad (1)$$

where ϕ is the one-lag autocorrelation parameter, assumed to be equal to 0.999, and $\varepsilon_{\omega,t}$ is a Gaussian white noise with mean zero and standard deviation $\sqrt{1-\phi^2}$.

The PV production and load profiles for each scenario ω ($P_{\omega,t}^{pv}$ and $P_{\omega,t}^{load}$) are obtained by applying the inverse transform method assuming a normal distribution, with the constraint that both profiles cannot be negative and that the difference between each profile and the corresponding forecast should not exceed 20% (in all the periods for the load and 75% of the periods for PV production).

B. Construction of the scenario tree

Each of the generated scenarios is assumed to be equiprobable and it is defined by the normalized difference between the PV production and the load.

The scenario tree is built by the consecutive application of the k -means clustering method, as described in e.g. [5].

As an additional alternative to reduce the number of final scenarios in the tree, a reduction of the centroids at each stage, based on their probability and the similarity to other centroids into the same stage was implemented [6]. Firstly, the probability of each centroid $\pi_s^{k_i}$ is compared with the average value of the probabilities of the others centroids present in the stage $\pi_{ref}^{k_i}$, if the value is lower than a defined percentage (20%

This work has received funding from the European Union's Horizon 2020 research and innovation programme under the Marie Skłodowska-Curie grant agreement No 675318 (INCITE).

in our simulations) of the reference value of probability, then the centroid is candidate to be removed:

$$\pi_{ref}^{k_i} = \left(\frac{\sum_{j \neq i}^K \pi_s^{k_j}}{K-1} \right) \quad (2)$$

$$\pi_s^{k_i} < \pi_{ref}^{k_i} \cdot 20\%$$

All the scenarios of the cluster represented by the removed centroid are reassigned to the closest cluster, according to the minimal value of the Euclidean distance weighted for $\pi_{ref}^{k_i}$:

$$\min \left[\pi_{ref}^{k_i} \cdot d(k_t^i, k_t^j) \right] \quad \forall i = 1 \dots K$$

$$d(k_t^i, k_t^j) = \sum_{t \in T_s} \|k_t^i - k_t^j\|_2 \quad (3)$$

C. Intraday decision-making procedure

The solution of the day-ahead recourse model provides multiple possible decisions at each stage following the first one (i.e., during the day). Therefore, for the actual operation, a decision-making procedure is needed for the choice of the most appropriate decision at each stage among those indicated by the stochastic problem solution, on the basis of the current PV generation and load.

At each stage, the decision-making procedure finds the scenario of the tree that is the most similar to the profile of the difference between PV generation and load in the previous 6 hours, on the basis of the Euclidean distance, among those scenarios directly connected to the tree node chosen in the previous stage. Then it decides the set point values of the battery power output for each 15-minutes time intervals of the following 6-hours.

III. NUMERICAL TESTS

The optimization procedures have been implemented in AIMMS Developer and tested by using the Cplex V12.8 MIP solver on 2-GHz processors with 8 GB of RAM, running 64-b Windows.

Table I compares the *OF* values of the stochastic solution of two models – the one simple battery representation and the one including the more refined kinetic battery model (KiBaM) – by using the scenarios trees obtained through the *k*-means clustering procedure (with 3 and 4 centroids) applied to 200 initial equiprobable PV generation and load profiles.

TAB. I SP SOLUTIONS AND METRICS FOR THE CASE WITH A 630 kWh BATTERY.

Battery model	Simple		KiBaM	
	3	4	3	4
<i>OF</i> (€)	38.02	38.25	61.67	61.80
<i>VSS</i> (€)	2.59	2.84	1.11	1.12
<i>EVPI</i> (€)	0.85	1.08	0.47	0.56
Number of scenarios in the tree	64	139	64	139
Solution time (s)	1.54	2.97	3.47	8.26

Table I also shows the Value of Stochastic Solution (*VSS*) and the Expected Value of Perfect Information (*EVPI*), which

are widely used metrics of the performance of using SP models [7].

VSS is the difference between the expected value solution (*EEV*) and the stochastic solution (i.e., the *OF* value). *EEV* is obtained by a two-step calculation: at first, the values of P_t^b for each *t* are given by the solution of the deterministic model obtained by replacing all random variables by their expected values; then, these P_t^b are set as a fixed parameters and *EEV* is given by the solution of the stochastic problem.

EVPI is the difference between the stochastic solution and the wait and see (WS) solution. WS is the expected value of the deterministic solutions of each scenario in the tree.

As expected, the higher the number of centroids the longer the computational effort due to the enlargement of the tree, as shown by the comparison of the solution times and the number of scenarios in the trees reported by Table I for *K*=3 and *K*=4. However, a more detailed clustering increases the *VSS*, even with an initial set of scenarios not very large with respect to the final dimensions of the tree.

Table I shows that the use of the more refined model of the battery increases both the *OF* values and the computation time, as expected.

Table II shows the average values of the following differences for the scenarios of the tree, for the initial set of 200 scenarios, and for 50 scenarios different from those of the previous set:

SP-MC difference between the *OF* values given by the intraday decision-making procedure and the Monte Carlo solution;

SP-WS difference between the *OF* values given by the intraday decision-making procedure and the deterministic solution.

TAB. II COMPARISON BETWEEN SP AND MONTE CARLO SIMULATIONS AND BETWEEN SP AND DETERMINISTIC SOLUTIONS (630 kWh BATTERY).

Battery model		Simple		KiBaM	
Number of centroids		3	4	3	4
Scenarios tree	SP – MC	-2.51	-2.55	-0.71	-0.69
	SP – WS	0.97	1.13	0.55	0.60
Set of initial scenarios	SP – MC	-2.05	-2.47	-0.23	-0.34
	SP – WS	5.17	2.70	1.81	1.70
Set of new scenarios	SP – MC	-2.28	-2.29	-0.26	-0.24
	SP – WS	4.85	4.84	1.91	1.92

The results of Table II show the advantage of using the SP and the benefit of a more accurate clustering procedure.

Finally, in order to show the performance of the SP approach using the additional alternative to reduce the number of final scenarios in the tree, the results of the numerical tests are summarized in Table III (*OF* values and metrics) and Table IV (comparison between SP and Monte Carlo simulations and between SP and deterministic solutions).

TAB. III SP SOLUTIONS AND METRICS FOR THE CASE WITH THE ADDITIONAL REDUCTION OF THE TREE.

Battery model	Simple		KiBaM	
Number of centroids	3	4	3	4
OF (€)	37.98	38.25	61.67	61.77
VSS (€)	2.55	2.77	1.08	1.12
EVPI (€)	0.82	1.08	0.45	0.53
Number of scenarios in the tree	53	137	53	137
Solution time (s)	1.05	2.94	2.45	7.33

TAB. IV. COMPARISON BETWEEN SP AND MONTE CARLO SIMULATIONS AND BETWEEN SP AND DETERMINISTIC SOLUTIONS (TREE REDUCTION).

Battery model		Simple		KiBaM	
Number of centroids		3	4	3	4
Scenarios tree	SP – MC	-2.53	-2.69	-0.77	-0.80
	SP – WS	0.87	1.09	0.49	0.56
Set of initial scenarios	SP – MC	-2.16	-2.30	-0.41	-0.48
	SP – WS	5.17	2.87	1.78	1.71
Set of new scenarios	SP – MC	-2.36	-2.56	-0.45	-0.49
	SP – WS	4.77	4.57	1.85	1.81

The results confirm the advantages of the SP. The use of 4 centroids increases the VSS, as expected, and, allows improved results.

IV. CONCLUSION

Multistage SP represents an attractive method for the day ahead scheduling in local energy systems and provides improved results with respect to the application of the Monte Carlo method.

The construction of the scenario tree needs to be addressed properly. The k -means clustering provides appropriate results even with a limited number of centroids. The computational effort is reasonable for the considered five-stage SP problem.

The SP approach is also applicable to models that include a detailed representation of the battery under the assumption that the mixed integer linear programming characteristics of the model are preserved.

REFERENCES

- [1] C. Orozco, A. Borghetti, S. Lilla, G. Pulazza, and F. Tossani, "Comparison Between Multistage Stochastic Optimization Programming and Monte Carlo Simulations for the Operation of Local Energy Systems," in *2018 IEEE International Conference on Environment and Electrical Engineering and 2018 IEEE Industrial and Commercial Power Systems Europe (EEEIC / I&CPS Europe), 12 -15 June, 2018*, 2018, vol. 737434, no. 737434, pp. 1–6.
- [2] F. Conte, S. Massucco, M. Saviozzi, and F. Silvestro, "A Stochastic Optimization Method for Planning and Real-Time Control of Integrated PV-Storage Systems: Design and Experimental Validation," *IEEE Trans. Sustain. Energy*, vol. 3029, no. LV, pp. 1–10, 2017.
- [3] S. Lilla, A. Borghetti, F. Napolitano, F. Tossani, D. Pavanello, D. Gabioud, Y. Maret, and C. A. Nucci, "Mixed integer programming model for the operation of an experimental low-voltage network," in *2017 IEEE Manchester PowerTech*, 2017, pp. 1–6.
- [4] G. J. Osório, J. M. Lujano-Rojas, J. C. O. Matias, and J. P. S. Catalão, "A new scenario generation-based method to solve the unit commitment problem with high penetration of renewable energies," *Int. J. Electr. Power Energy Syst.*, vol. 64, pp. 1063–1072, 2015.
- [5] H. Pranevicius and K. Šutiene, "Scenario tree generation by clustering the simulated data paths," in *Proceedings 21st European Conference on*

Modelling and Simulation ECMS 2007, 2007, pp. 203–208.

- [6] R. Barth, L. S. oder, C. Weber, H. Brand, and D. J. Swider, "Methodology of the Scenario Tree Tool," *Inst. Energy Econ. Ration. Use Energy Univ. Stuttgart*, vol. 2, no. January 2006, pp. 1–27, 2006.
- [7] L. F. Escudero, A. Garín, M. Merino, and G. Pérez, "The value of the stochastic solution in multistage problems," *Top*, vol. 15, no. 1, pp. 48–64, 2007.

A fault detection and localization method for LV distribution grids

Nikolaos Sapountzoglou*, ESR 4.2, Bertrand Raison* and Nuno Silva**

Abstract—A fault detection and localization method for low voltage (LV) distribution grids is described in this paper. The details of a real case LV grid were provided by Efacec. Single-phase and three-phase short circuit (SC) faults were studied in different hours during the day (at 10 and 16 [hours]) and for various fault resistance values (0.1, 1, 5 and 10 [Ω]). A method based on the form of the voltage curves during the steady state of the faults was developed. Simulations were run in the MATLAB/Simulink environment to validate the method.

Index Terms—Fault detection, Fault localization, LV grid

I. INTRODUCTION

For the purpose of this study, a real case semi-rural radial LV grid of Portugal was used. It is a three-phase-four-wire grid with a solidly grounded neutral, consisting of three main feeders and a total of thirty three nodes with 15 microgenerators (single-phase PV installations) and twenty eight single-phase loads. The single line diagram of the LV distribution grid is presented in Fig. 1 along with the available measurements and the fault locations under study.

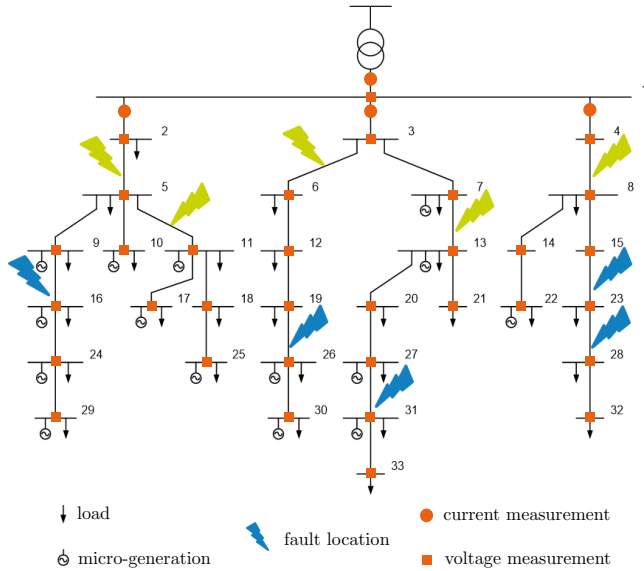


Fig. 1: Single line diagram of the LV grid with the SC fault cases.

Document submitted July 4, 2018.

This project has received funding from the European Union's Horizon 2020 research and innovation programme under the Marie Skłodowska-Curie grant agreement No 675318 (INCITE).

*N. Sapountzoglou and B. Raison are with the Université Grenoble Alpes, CNRS, Grenoble INP (Institute of Engineering), G2Elab, 38000 Grenoble, France. (email: nikolaos.sapountzoglou@g2elab.grenoble-inp.fr ; bertrand.raison@g2elab.grenoble-inp.fr)

**N. Silva is with Efacec, Maia, Portugal (email: nuno.silva@efacec.com)

Eleven different types of conductors connect the nodes with each other with a maximum length of 210 [m]. The microgeneration and load profiles for one day are given in Fig. 2.

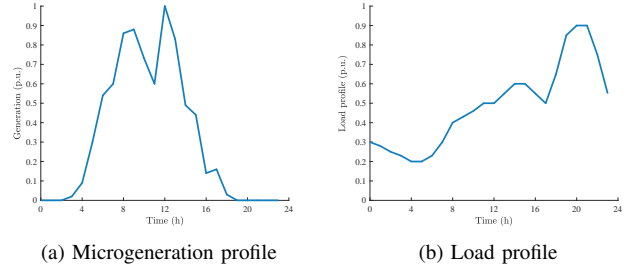


Fig. 2: Grid characteristics

II. FAULT DETECTION

For the detection of a fault occurrence, current measurements at the transformer level were used. In order to detect an anomaly, the derivatives of the phase currents were monitored. A sudden increase of the absolute value of the derivative of the current, indicated the fault occurrence. The absolute value was used because in some fault cases with high fault resistance (10 [Ω]), a small decrease instead of the expected increase in the current was observed. Moreover, the algorithm is able to detect evolving faults, a typical case being the evolution of a single-phase to ground fault into a three-phase fault, by tracking the behavior of the current in all three phases. Once the fault is detected, the fault localization part of the algorithm is initiated. The steady state of the fault is analyzed.

III. FAULT LOCALIZATION

The fault localization algorithm is divided in three steps: a) faulty branch localization, b) faulty sector localization and c) fault location calculation. The branch of a grid is defined as a unique line path from the transformer to each terminal node (branch 1: from 1 to 29). At the same time, the sector is defined as the part of the grid between two available measurements. In this case, since voltage measurements are available at each node, the sector is the line connecting two adjacent nodes (sector 1: from 1 to 2).

A. Faulty branch localization

The faulty branch localization is split in two parts. In order to identify the faulty branch of the grid, current measurements at the beginning of each feeder were necessary. The use of voltage measurements alone could lead to

false alarms due to misslocalization of a fault (especially in high fault resistance cases where the voltage drop is not significant and load contribution may conceal the fault occurrence). Hence, the first part consists in identifying the faulty feeder. Once again, a sudden increase of the absolute value of the derivative of the phase current was used. When the faulty feeder is identified, the algorithm proceeds with the localization of the branch within the selected feeder. The branch to which the node with the lowest voltage belongs was considered as the faulty branch. Finally, it was observed that among the available measurements (phase and symmetrical components) the positive sequence component of the voltage was the most reliable.

B. Faulty sector localization

The positive sequence component of the voltage across a faulty branch is presented in Fig. 3. In this example, the fault is a three-phase SC of 1 $[\Omega]$ fault resistance occurring at 10h01m00s; the fault is located in the 5th branch (from node 1 to node 30 in Fig. 1) and in the middle of the 5th sector (between the nodes 19 and 26). As stated before, the faulty branch is the one with the highest voltage drop within the feeder.

The localization of the sector under fault is achieved through the comparison of two consecutive voltage measurements, ideally corresponding to two adjacent nodes. From the linearly interpolated curve of the voltage in Fig. 3, it can be observed that the voltage constantly decreases up to the next measurement after the point of fault occurrence. After, the faulty sector (presented with a red line in Fig. 3) the curve's slope decreases to a value close to zero. Extreme cases where the voltage increases again after the faulty sector were also noticed.

In order to cover the vast majority of the fault cases, the two following criteria were developed in order to detect the faulty sector:

- 1) if the difference between two consecutive voltage measurements is positive, signifying a change in the sign of the slope, then the previous sector is the one under fault and
- 2) if the absolute value of the difference between two adjacent voltage measurements is the lowest within the branch, signifying a stabilization of the curve, then the previous sector is the one under fault.

C. Fault location calculation

After both the branch and the sector under fault are identified, the only thing left is to calculate where inside the sector has the fault occurred. Returning to Fig. 3, by linearly extrapolating the lines consisting the previous and the following sectors of the one under fault, it becomes possible to find their intersection point. Therefore, this point corresponds to the location of the fault. For the example of Fig. 3, the fault was found to be located 405 [m] away from the transformer while in reality it was located at 410 [m]. The deviation of the method in locating the fault was, in this case, 5 [m].

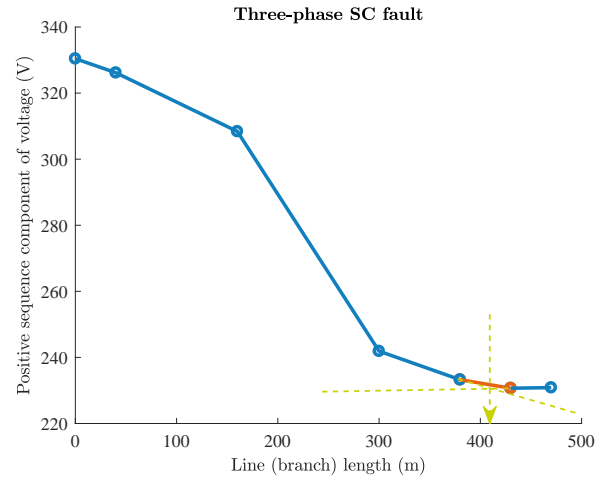


Fig. 3: Voltage profile snapshot across a faulty branch (between nodes 19 and 26) for a SC three-phase fault of 1 $[\Omega]$ fault resistance at 10h02m01s.

IV. RESULTS

The MATLAB/Simulink environment was used for the simulations and the development of the method. Two categories of faults were studied: a) single-phase to ground faults and b) three-phase faults. Simulations with faults occurring at two different times during a day were executed: a) at 10h01m00s (73% of microgeneration) and b) at 16h01m00s (14% of microgeneration). Additionally, for each of the above cases four types of fault resistance were investigated: a) 0.1 $[\Omega]$, b) 1 $[\Omega]$, c) 5 $[\Omega]$ and d) 10 $[\Omega]$.

The method was found to be almost 100% accurate (95,56% for single-phase faults and 100% for three-phase faults) in detecting the fault and identifying the faulty feeder, branch and sector for faults located relatively far from the transformer (blue markers in Fig. 1). For faults located closer to the beginning of the feeder (green markers in Fig. 1), where faulty sectors belong to multiple branches, the method was 50% accurate. This error derives from the fact that the wrong branch was selected for the identification of the faulty sector. Another conclusion that was drawn is that the precision of the method decreases with the increase of the fault resistance. Additionally, the level of participation of microgeneration does not seem to affect the results of the method. Finally, due to the nature of the method -linear extrapolation- at least three consecutive measurements inside a branch are needed to identify a faulty sector, meaning that faults can not be correctly identified if they are found in the first or the last sector.

V. CONCLUSION & FUTURE WORK

A fault detection and localization method was developed for a real LV distribution grid of Portugal provided by Efaced. Further analysis is needed in order to increase its accuracy for the faults close to the beginning of the feeder. An alternative to the linear interpolation method for the creation of the voltage curve, could be the use of the least squares method. As a last step, measurement perturbations will be implemented to test the sensitivity of the method.

Stochastic Optimal Power Flow in Distribution Grids under Uncertainty from State Estimation

Miguel Picallo, Adolfo Anta and Bart De Schutter

I. INTRODUCTION

The increase of distributed generation and controllable loads presents many advantages for the distribution grid but at the same time requires new techniques to guarantee a proper operation. To face these new challenges, optimal power flow (OPF) strategies from transmission grids are being adapted to distribution grids.

The OPF is dependent on the state of the grid (voltages, currents, loads, etc.), which at the distribution level is only partially known. While enough sensors are usually available in transmission grids, this is not the case for distribution grids, where state estimation (SE) algorithms [AE04] are necessary. These SE algorithms provide an estimation of the variables of interest, with a certain degree of uncertainty. Ignoring this uncertainty in SE could lead to voltage limit violations. Some papers introduce chance constrained optimization methods to account for the uncertainty in the loads and generation [SWML15], [DBS17].

II. STATE ESTIMATION

We consider a standard SE algorithm [AE04] that provides an unbiased estimation of the network voltages $V_{\text{est}} \in \mathbb{C}^N$, $V_{\text{est,rect}} = [\Re\{V_{\text{est}}\}^T, \Im\{V_{\text{est}}\}^T]^T \in \mathbb{R}^{2N}$ in rectangular coordinates, and a covariance matrix representing its uncertainty $\Sigma_{\text{est,rect}} \in \mathbb{R}^{2N \times 2N}$ [PAPS18]. This uncertainty is mainly caused by sensor noise and uncertainty in load predictions. The true voltages before applying the OPF are:

$$V_{\text{prev,rect}} \sim \mathcal{N}(V_{\text{est,rect}}, \Sigma_{\text{est,rect}}) = V_{\text{est,rect}} + \Sigma_{\text{est,rect}}^{\frac{1}{2}} \mathcal{N}(0, I_d) \quad (1)$$

III. STANDARD OPTIMAL POWER FLOW

In this paper, we consider as controllable elements the distributed generation sources at the distribution level $\{(P_i, Q_i) \mid i \in \mathcal{V}_{\text{ren}}\}$, where \mathcal{V}_{ren} denotes the set of nodes with distributed renewable energy sources; and the set points of the voltage tap changers for every phase ϕ in the transformers $a_{\text{tap},\phi} \in \{a_{\text{tap,min}}, \dots, a_{\text{tap,max}}\}$. For simplicity, the objective is to minimize the total amount of energy required from the substation S_{src} . The safety conditions are given by the limits for the voltage magnitudes $|V|$:

This project has received funding from the European Union's Horizon 2020 research and innovation programme under the Marie Skłodowska-Curie grant agreement No 675318 (INCITE).

M. Picallo and B. De Schutter are with the Center for Systems and Control, Delft University of Technology, The Netherlands {m.picallocruz, b.deschutter}@tudelft.nl

A. Anta is with Austrian Institute of Technology Adolfo.Anta@ait.ac.at

$$\text{Objective: } \min \sum_{\phi} P_{\text{src},\phi} + Q_{\text{src},\phi} \quad (2a)$$

Constraints:

Power flow:

$$\begin{bmatrix} S_{\text{src}} \\ S \end{bmatrix} = \text{diag} \left(\begin{bmatrix} V_{\text{src}} \\ V \end{bmatrix} \right) \bar{Y}(a_{\text{tap}}) \begin{bmatrix} \bar{V}_{\text{src}} \\ \bar{V} \end{bmatrix} \quad (2b)$$

$$\text{Tap changers: } \forall \phi \in \{1, 2, 3\} \ a_{\text{tap},\phi} \in \{a_{\text{tap,min}}, \dots, a_{\text{tap,max}}\} \quad (2c)$$

Available energy: $\forall i \in \mathcal{V}_{\text{ren}}$

$$P_{\text{min},i} \leq P_i \leq P_{\text{max},i}, \ Q_{\text{min},i} \leq Q_i \leq Q_{\text{max},i} \quad (2d)$$

$$\text{Voltage limits: } \forall i \in \{1, \dots, N\} \ |V|_{\text{min}} \leq |V_i| \leq |V|_{\text{max}} \quad (2e)$$

where $|V|_{\text{max}}, |V|_{\text{min}}$ denote the voltage magnitude limits, $P_{\text{max},i}, Q_{\text{max},i}, P_{\text{min},i}, Q_{\text{min},i}, |S|_{\text{max},i}$ denote the available energy limits at node i , and $Y(a_{\text{tap}})$ denotes the admittance matrix as a function of the vector of voltage tap changers a_{tap} . The variables to optimize are then the power supplied by the substation and the renewable energy sources $S_{\text{src}}, \{(P_i, Q_i) \mid i \in \mathcal{V}_{\text{ren}}\}$, the voltage tap changers a_{tap} , and the voltages V and V_{src} . Among the variables, the control elements are $a_{\text{tap}}, \{(P_i, Q_i) \mid i \in \mathcal{V}_{\text{ren}}\}$ and V_{src} , while S_{src} and V are determined by the constraints. The loads at the rest of the nodes $\{(P_i, Q_i) \mid i \notin \mathcal{V}_{\text{ren}}\}$ are inputs to the OPF problem, and are typically measured or estimated.

IV. STOCHASTIC OPTIMAL POWER FLOW

There are some problems with the OPF representation in (2): (i) The power flow equation in (2b) is nonlinear and nonconvex and thus difficult to handle. (ii) In (2b), both all voltages and the loads in the nodes other than the substation and the renewable sources: $\{(P_i, Q_i) \mid i \notin \mathcal{V}_{\text{src}} \cup \mathcal{V}_{\text{ren}}\}$, where \mathcal{V}_{src} denotes the set of nodes in the source bus. known. (iii) There is a degree of uncertainty in the SE with covariance matrix $\Sigma_{\text{est,rect}}$, that needs to be considered in the voltage limits in (2e).

A. Transformer Approximation

In order to include the tap changers more efficiently and to simplify $Y(a_{\text{tap}})$ in (2b), we assume electrical isolation at the transformers and thus consider different subsystems related by the tap changers equations similar to [RZDG16]:

$$\begin{bmatrix} S_{\text{src}} \\ S \end{bmatrix} = \text{diag} \left(\begin{bmatrix} V_{\text{src}} \\ V \end{bmatrix} \right) \bar{Y}_{\text{isol}} \begin{bmatrix} \bar{V}_{\text{src}} \\ \bar{V} \end{bmatrix} \quad (3)$$

$$V_{\text{tf2}} = \text{diag}(a_{\text{tap}}) V_{\text{tf1}}, \ 0 = S_{\text{tf2}} + S_{\text{tf1}}$$

where V_{tf} correspond to the nodes of the transformer for each subsystem, Y_{isol} is the admittance with isolated subsystems. We also consider a continuous tap changer: $\phi, a_{\text{tap},\phi} \in [a_{\text{tap,min}}, a_{\text{tap,max}}]$.

B. Power Flow Approximation

We use a first-order linear approximation of (2b) around the estimated voltage states V_{est} :

$$\begin{aligned} \begin{bmatrix} \Delta S_{\text{src}} \\ \Delta S \end{bmatrix} &= \text{diag} \left(\begin{bmatrix} \Delta V_{\text{src}} \\ \Delta V \end{bmatrix} \right) \bar{Y}_{\text{isol}} \begin{bmatrix} \bar{V}_{\text{src,prev}} \\ \bar{V}_{\text{est}} \end{bmatrix} \\ &+ \text{diag} \left(\begin{bmatrix} V_{\text{src,prev}} \\ V_{\text{est}} \end{bmatrix} \right) \bar{Y}_{\text{isol}} \begin{bmatrix} \Delta \bar{V}_{\text{src}} \\ \Delta \bar{V} \end{bmatrix} \\ \Delta V_{\text{tf2}} &= \text{diag}(a_{\text{tap,prev}}) \Delta V_{\text{tf1}} + \text{diag}(V_{\text{tf1,prev}}) \Delta a_{\text{tap}} \\ 0 &= \Delta S_{\text{tf1}} + \Delta S_{\text{tf2}} \end{aligned} \quad (4)$$

where for every $x = \{S, V, a_{\text{tap}}\}$, $\Delta x = x - x_x$ represent the change of values after the optimization process.

Remark 1: We consider that the optimization process is fast enough, so that the loads remain constant: $\Delta S_i = 0$ for $i \notin \mathcal{V}_{\text{src}} \cup \mathcal{V}_{\text{ren}} \cup \mathcal{V}_{\text{tf1}} \cup \mathcal{V}_{\text{tf2}}$, where $\mathcal{V}_{\text{tf1}}, \mathcal{V}_{\text{tf2}}$ denote the set of nodes on the transformer. This allows to bypass the lack of load measurements.

C. Stochastic Voltage Limits

Since we have a SE with uncertainty (1), the voltage after the optimization step V , $V_{\text{rect}} = [\Re\{V\}^T, \Im\{V\}^T]^T$ is:

$$V_{\text{rect}} \sim \mathcal{N}(\Delta V_{\text{rect}} + V_{\text{est,rect}}, \Sigma_{\text{est,rect}}) \quad (5)$$

Then, instead of a deterministic voltage limit constraint like (2e), we have a stochastic one:

$$P(|V|_{\min} \leq |V_i| \leq |V|_{\max}) \geq \beta \quad \forall i \quad (6)$$

where β is a threshold probability level. We use the following theorem to reformulate (6):

Theorem 1: For all $\beta \in (0, 1)$, there exists α such that if the following constraints holds for all i :

$$\begin{aligned} &(\Re\{\Delta V_i\} + \Re\{V_{\text{est},i}\} \pm \alpha(\Sigma_{\text{est,rect},\Re})_{i,i}^{\frac{1}{2}})^2 \\ &+ (\Im\{\Delta V_i\} + \Im\{V_{\text{est},i}\} \pm \alpha(\Sigma_{\text{est,rect},\Im})_{i,i}^{\frac{1}{2}})^2 \leq |V|_{\max}^2 \\ &(\Re\{\Delta V_i\} + \Re\{V_{\text{est},i}\} \pm \alpha(\Sigma_{\text{est,rect},\Re})_{i,i}^{\frac{1}{2}}) \frac{\Re\{V_{\text{est},i}\}}{|V_{\text{est},i}|} \\ &+ (\Im\{\Delta V_i\} + \Im\{V_{\text{est},i}\} \pm \alpha(\Sigma_{\text{est,rect},\Im})_{i,i}^{\frac{1}{2}}) \frac{\Im\{V_{\text{est},i}\}}{|V_{\text{est},i}|} \geq |V|_{\min} \end{aligned} \quad (7)$$

then (6) is satisfied. We use \pm to denote all possible combinations to represent all constraints.

Furthermore, α can be found using standard tables for Gaussian distributions by choosing α such that

$$P(|\tilde{\omega}| \geq \alpha) \leq \frac{1-\beta}{4}, \text{ for } \tilde{\omega} \sim \mathcal{N}(0, 1) \quad (8)$$

D. Final OPF

Using Thm. 1 we can rewrite (6) into a convex deterministic constraint, so that it can be integrated into our OPF problem:

$$\text{Objective: } \min \sum_{\phi} P_{\text{src},\phi} + Q_{\text{src},\phi} \quad (9a)$$

$$\text{Constraints:} \quad (9b)$$

$$\text{Power flow: (4)} \quad (9b)$$

$$\text{Tap changers: } a_{\text{tap},\phi} \in [a_{\text{tap,min}}, a_{\text{tap,max}}], \quad \forall \phi \in \{1, 2, 3\} \quad (9c)$$

$$\begin{aligned} \text{Available energy:} \\ P_{\min,i} \leq \Delta P_i + P_{\text{prev},i} \leq P_{\max,i}, \quad \forall i \in \mathcal{V}_{\text{ren}} \\ Q_{\min,i} \leq \Delta Q_i + Q_{\text{prev},i} \leq Q_{\max,i}, \quad \forall i \in \mathcal{V}_{\text{ren}} \end{aligned} \quad (9d)$$

$$\text{Voltage limits: (7)} \quad (9e)$$

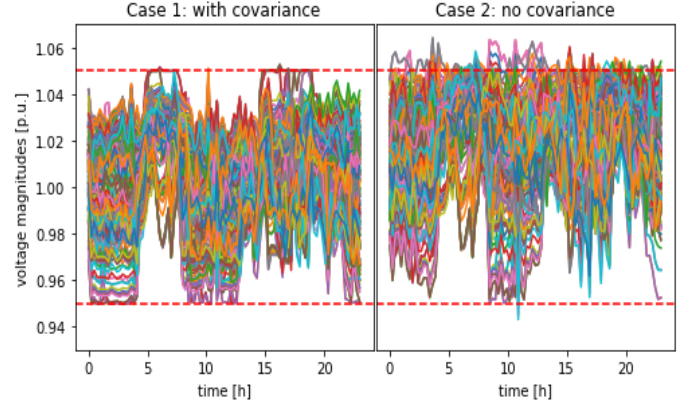


Fig. 1: Voltage magnitude $|V|$ profiles for all nodes along the day for case 1 and 2: with and without taking into account the covariance of the SE for the OPF respectively. The red dashed lines represent the limits.

where now the variables to control are Δa_{tap} , $\{(\Delta P_i, \Delta Q_i) \mid i \in \mathcal{V}_{\text{ren}}\}$ and ΔV_{src} , while ΔP_{src} , ΔQ_{src} and ΔV are determined by the constraints. All previous values before the optimization step, $a_{\text{tap,prev}}$, $P_{\text{prev},i}$, $Q_{\text{prev},i}$, $S_{\text{prev},i}$, are stored from the control step before the current one, and V_{est} and $\Sigma_{\text{est,rect}}$ are given by the SE.

V. CASE STUDY

A simulation of 24 hours with 15 min intervals is run on the 123-bus test feeder available online [Ker91] to test the effectiveness of the methodology.

We have compared the resulting voltage magnitudes when controlling the transformer and the introduced energy in two cases: in case 1, we take the uncertainty into account, using the covariance to ensure the voltage limit constraints; while in case 2, we are using the voltage estimates as if they were the true values, without taking into account the covariance. It can be observed in Fig. 1 that case 1, using the covariance, performs much better than case 2 in controlling the voltage magnitudes within their limits.

REFERENCES

- [AE04] A. Abur and A. G. Exposito. *Power System State Estimation: Theory and Implementation*. CRC Press, 2004.
- [DBS17] E. Dall'Anese, K. Baker, and T. Summers. Chance-constrained AC optimal power flow for distribution systems with renewables. *IEEE Transactions on Power Systems*, 32(5):3427–3438, Sept 2017.
- [Ker91] W.H. Kersting. Radial distribution test feeders. *IEEE Transactions on Power Systems*, 6(3):975–985, 1991.
- [PAPS18] M. Picallo, A. Anta, A. Panosyan, and B. De Schutter. A two-step distribution system state estimator with grid constraints and mixed measurements. In *IEEE Power Systems Computation Conference*, 2018. to appear, arXiv:1703.10815.
- [RZDG16] B. A. Robbins, H. Zhu, and A. D. Domnguez-Garcia. Optimal tap setting of voltage regulation transformers in unbalanced distribution systems. *IEEE Transactions on Power Systems*, 31(1):256–267, Jan 2016.
- [SWML15] T. Summers, J. Warrington, M. Morari, and J. Lygeros. Stochastic optimal power flow based on conditional value at risk and distributional robustness. *International Journal of Electrical Power & Energy Systems*, 72:116 – 125, 2015. The Special Issue for 18th Power Systems Computation Conference.

A multi-period Optimal Power Flow scheme for Low Voltage Distribution Networks

ESR 4.4 Advanced functionalities for the future Smart Secondary Substation

Konstantinos Kotsalos, Nuno Silva, Ismael Miranda and Helder Leite

Abstract—This work aims to propose a three phase multi-period Optimal Power Flow (OPF) framework for the coordination of multiple Distributed Energy Resources (DER) in low voltage distribution grids. The proposed scheme considers forecasted information for load and renewable generation, in addition to the demand flexibility, and derives possible scheduling of multiple controllable assets such as battery storage system (BSS), electric vehicles and deferrable loads. The proposed methodology leans on a multiperiod Optimal Power Flow scheme, which is addressed either as a non-linear optimization problem or a linear one in case binary control variables are assigned. In this document a brief description of the BSS temporal model is presented. The main target of this tool is to take advantage of the flexibility given by DER to ensure cost-effective and within statutory limits operation of the LV grid.

I. INTRODUCTION

The increasing integration of DER along the distribution networks pose several technical challenges, which can be addressed by the active management of such resources. Distribution System Operators (DSOs) are currently increasing the observability and controllability of the grids, envisioning the active management of the DERs for ancillary services, throughout new operation stages.

Recent studies have addressed the possibility of considering Low Voltage (LV) controllable assets beyond DSO assets, such a distributed battery storage system, controllable loads under demand response schemes and micro-generation units [1]. Particular focus has been given in aggregating flexible resources connected along the LV grid to support the operation of MV, by considering the LV grid as a flexible cluster [2]. Advanced methodologies need to be implemented to determine control actions related to controllable DER, that can techno-economically improve distribution networks operation delivering benefits to residential users.

Previous implementations were focused on the scheduling of the controllable units based on a sequential scheme [3]. This tool provided a scheduling of the resources ensuring voltages within the admissible limits.

In this work, a description of the structured DER models is presented along with their temporal coupling along the optimization horizon. A fully coupled multi-period OPF scheme is proposed considering the multiphase unbalanced nature of the LV grids. The contribution of this work is to propose a flexible operational tool, which provides support to the DSO for the efficient coordination of DER in a centralized manner.

II. PROBLEM STATEMENT

In this section, the multiperiod three-phase OPF is stated for an horizon of operational planning H_t . The objective function

$f(X)$ is to minimize the operating costs assigned with all the controllable assets providing their coordination, based on their availability. Furthermore, an additional storage degradation cost, can be attributed to the objective function as an affine function expressed with a linear combination of the storage powers.

In this work all buses are considered to have three terminals, where each one represents the phase connection point, a, b, c . The latter implies that for bus j , the voltage magnitude is given by the real vector $v_j \in \mathbb{R}^3$, $v_j = [v_{j,a}, v_{j,b}, v_{j,c}]^T$, and accordingly the voltage angles by the real vector $\theta_j \in \mathbb{R}^3$. For the multiperiod formulation, assuming that the decision variables at the time instant τ is correspond to the vector x_τ , which is defined as follows:

$$x_\tau = \begin{bmatrix} \Theta \\ \mathcal{V} \\ P_g \\ Q_g \end{bmatrix}_\tau, \forall \tau \in \mathcal{T}, x_\tau \in \mathbb{R}^{(2*3n_b+2*n_c)} \quad (1)$$

where n_b refer to the number of buses and n_c the controllable units. The real vector $\Theta = [\theta_1, \theta_2, \dots, \theta_{n_b}]^T$ correspond to the angles of each bus, and respectively $\mathcal{V} \in \mathbb{R}^{3*n_b}$ to the voltage magnitudes, $\mathcal{V} = [v_1, v_2, \dots, v_{n_b}]^T$ $v_j = [v_{j,a}, v_{j,b}, v_{j,c}]^T$. The sets $\mathcal{N}, \mathcal{J}, \mathcal{T}$, denote the buses, branches and the horizon of the multi-period scheme. Let us consider the set of controllable assets $\mathcal{U} := \{u_1, \dots, u_{n_c}\}$, described by the control vector u , comprised by active and reactive power set points, P_g, Q_g .

Therefore, for the overall optimization problem the decision variables correspond to the matrix $X = [x_0, x_1, \dots, x_{H_t}]^T$.

$$\min f(X) = \min_u \sum_{\tau=1}^{H_t} \sum_k^{n_b} ([c_{n_c}(\tau)]^T \cdot u_{k,\tau}) \quad (2)$$

subjected to

$$F_j(x_\tau, u_\tau) = 0 \quad \forall j, \tau \in \mathcal{N}, \mathcal{T} \quad (3a)$$

$$h_i(x_\tau, u_\tau) \leq 0 \quad \forall i, \tau \in \mathcal{J}, \mathcal{T} \quad (3b)$$

$$V_{\min} \leq v_j(x_\tau) \leq V_{\max} \quad \forall i, \tau \in \mathcal{N}, \mathcal{T} \quad (3c)$$

$$h_\xi(x_\tau, u_\tau) \leq 0 \quad \forall \xi, \tau \in \mathcal{U}, \mathcal{T} \quad (3d)$$

$$g_\xi(x_\tau, u_\tau) \leq 0 \quad \forall \xi, \tau \in \mathcal{U}, \mathcal{T} \quad (3e)$$

where the constraints in (3a) set the power balances at each bus of the network; the second constraint poses the nonlinear constraint for the constrained lines; the boxed constraint in (3c) to respect all nodal voltages to range strictly within the admissible bounds. The constraints (3d)-(3e), correspond to the operational limits of the controllable DER. The gradient and Hessian matrix of the objective function and the non-linear constraints are provided to the optimization solver, by expanding the calculations presented in [4].

There is a particular concern on its performance, since the formulation of the multi-temporal planning of operation scheme

will have augmented convergence time due to the large scaling of the problem, in addition to the linkup of intertemporal constraints. More analytically, flexible assets such as battery storage systems, EVs and controllable loads, induce the capability to commit certain amount of energy and release it at another one. The complexity of the multiperiod OPF scheme increases proportionally to the number of buses -including each corresponding phase- $n'_b = 3 \cdot n_b$, the number of controllable sources as well as the number of time steps incorporated in the horizon time H_t .

The proposed scheme in case of assigned binary control variables resorts to the equivalent multiperiod optimization problem by setting only power balance constraints. An additional step is added, to validate that the control set points lead to statutory limits at all time steps. The following section, provides the temporal description of the Battery Storage System (BSS) along the horizon optimization.

A. Battery Storage System (BSS)

1) *Model and operational constraints*: The Battery Storage System (BSS) is composed by the energy storage model and an additional rule based control for its active and reactive power. The energy storage is based on a first-order system, which can follow two states the charging and discharging mode. At the first one, the system increases its required consumption in order to get charged, while it injects power the grid during its discharging mode. The stored energy at the upcoming step will be given by

$$e_{(t+1)} = \begin{cases} \alpha e_{(t)} + T_s \eta_1 p_{(t)} & \text{if } p_{(t)} \geq 0 \\ \alpha e_{(t)} + T_s (1/\eta_2) p_{(t)} & \text{if } p_{(t)} < 0 \end{cases} \quad (4)$$

where e_t is the stored energy at the time step t , α is the drain rate of the system (i.e. for ideal BSS is 1), T_s is the sampling time that the system is traced, η_1, η_2 correspond o the charging and discharging efficiency, accordingly.

There are some operational constraints for both operation modes of the j -th BSS as follows:

$$\underline{e} \leq e_{(t)} \leq \bar{e} \quad (5a)$$

$$\underline{p} \leq p_{(t)} \leq \bar{p} \quad (5b)$$

$$|p_{(t)} - p_{(t-1)}| \leq p_{rate} \quad (5c)$$

where constraint 5a refers to the minimum and maximum energy of the system, 5b poses the minimum and maximum limits of power charging or discharging, and 5c sets the power consumption or injection rate. Including the power rate constraint, the power consumed or injected at the next (simulation) step is determined as follows:

$$p_{(t)} = \begin{cases} p_{t-1} + \text{sign}(p_t - p_{t-1}) p_{rate} & \text{if } |p_t - p_{t-1}| > p_r \\ p_t & \text{else} \end{cases} \quad (6)$$

The BSS can be dis/-charged following two different strategies either following a droop control proportional to the PCC voltage, or depending the its State of Charge (SoC)

$$p_{(t)} = \begin{cases} \underline{p} & \text{if } 0 < e_t < \bar{e} \wedge p_\xi < \underline{p} \\ \bar{p} & \text{else if } 0 < e_t < \bar{e} \wedge p_\xi > \bar{p} \\ p_\xi & \text{else } (e_t = 0 \wedge p_\xi \leq 0) \vee (e_t = \bar{e} \wedge p_\xi \geq \bar{p}) \end{cases} \quad (7)$$

where p_ξ a possible active control signal. Accordingly, the BSS might have additional control functionalities for each reactive

power output control. This can be implemented by the following function that determines the q_{BSS} :

$$q_{BSS} = \begin{cases} p_{(t)} \cdot \tan(\cos^{-1} * (\theta)) & \text{if } \cos(\theta) = \text{constant} \\ \text{droop}(Q, v_{j,\phi}, \text{param.}) & \text{else if droop= ON} \\ 0 & \text{else} \end{cases} \quad (8)$$

2) *Decision Variables*: As described above the BSS present a time-flexible asset that is capable injecting or consuming power to the network from one step to the other. Therefore its flexibility depends on taking advantage of absorbing or injecting power at certain periods, fact which needs to be incorporated to operational planning horizon. Assuming n_{bs} connected along the network, the branch function 4 can be rewritten in matrix format capturing both operating modes as follows:

$$e_{(t+1)} = \mathbf{I}^{2n_s} e_{(0)} + \underbrace{\Delta T_s [\text{diag}\{n_{dis}\} \quad \text{diag}\{1/n_{ch}\}]}_{\Lambda} \cdot \underbrace{\begin{bmatrix} p_{dis} \\ p_{ch} \end{bmatrix}}_{p_s(t)} \quad (9)$$

The energy stored to each battery storage system towards the evolution among the time horizon H_t can expressed as the vector $[E] = [e(0), \dots, e(H_t - 1)]^T$:

$$[E] = \begin{bmatrix} \mathbf{I}^{2n_s} \\ \vdots \\ \mathbf{I}^{2n_s} \end{bmatrix} e_{(0)} + \begin{bmatrix} \Lambda & 0 \\ \vdots & \ddots \\ \Lambda & \dots & \Lambda \end{bmatrix} \begin{bmatrix} p_s(0) \\ \vdots \\ p_s(H_t - 1) \end{bmatrix} \quad (10)$$

Therefore, the control variable for each battery storage system corresponds to the vector $p_s(t)$. Additional options are posed for the BSS, to include target point of the SoC at the end of the horizon time. The temporal expression for the Electric Vehicles is rather similar to the one described for the BSS.

B. Controllable Loads

Concerning the end-users' flexibility several concerns can be asserted. For the sake of simplicity hereby, the operation of the controllable loads can be deferrable loads at some certain time periods. Therefore, such loads can provide the flexible amount of active power as. More sufficiently for residential users is to assign loads which can be shifted. Due to lack of space, the model is not thoroughly discussed in this document.

III. CONCLUSIONS

Currently, the work is focused on the improvement of the convergence of the proposed methodology. Additional objective terms will be examined to verify the impact on the operational tool. The proposed scheme will be compared with an approximative one which considers solely power balance equations. Future tasks will address the incorporation of uncertainties - related to loads and PV forecasts- in the current scheme.

REFERENCES

- [1] P. C. Olival, A. G. Madureira, and M. Matos, "Advanced voltage control for smart microgrids using distributed energy resources," *Electric Power Systems Research*, vol. 146, pp. 132-140, 2017.
- [2] B. D. Tavares, J. Sumaili, F. J. Soares, A. G. Madureira, and R. Ferreira, "Assessing the impact of demand flexibility on distribution network operation," in *IEEE Manchester PowerTech*, 2017, Conference Proceedings, pp. 1-6.
- [3] K. Kotsalos, N. Silva, I. Miranda, and H. Leite, "Scheduling of operation in low voltage distribution networks with multiple distributed energy resources," in *CIREN Workshop 2018*, Conference Proceedings.
- [4] R. D. Zimmerman, "AC power flows, generalized OPF costs and their derivatives using complex matrix notation," MATPOWER, Tech. Rep., 2010.